Palaeogeography, Palaeoclimatology, Palaeoecology 675 (2025) 113073

Contents lists available at ScienceDirect

Palaeogeography, Palaeoclimatology, Palaeoecology

journal homepage: www.elsevier.com/locate/palaeo

Phenotypic diversity of brown trout (*Salmo trutta* L.) during the late Upper Pleistocene and Early Holocene in the glacial refugium of Iberia

Ambra D'Aurelio [a,*], Lucía Agudo Pérez [b], Lawrence G. Straus [b,c], Manuel R. González Morales [d], Arturo Morales-Muñiz [e], Jerome Primault [f], Jean-Marc Roussel [g], Laurence Tissot [h], Stephane Glise [a], Frederic Lange [a], Camille Riquier [a], Michel Barbaza [i], Eduardo Berganza [j], José Luis Arribas [k], Pablo Arias [d], Aurélien Simonet [l], Ana B. Marín-Arroyo [b], Joelle Chat [a], Françoise Daverat [a]

[a] Université de Pau et des Pays de l'Adour, INRAE, UMR ECOBIOP, Saint-Pée-sur-Nivelle, France
[b] Grupo I+D+I EvoAdapta, Dpto. de Ciencias Históricas, Universidad de Cantabria, Santander, Spain
[c] Department of Anthropology, MSC01 1040, University of New Mexico, Albuquerque, NM 87131-0001, USA
[d] Instituto Internacional de Investigaciones Prehistóricas de Cantabria, Universidad de Cantabria, Gobierno de Cantabria, Santander, Spain
[e] Laboratorio de Arqueozoología (LAZ-UAM)-Universidad Autónoma de Madrid, Darwin, 2, Madrid, Spain
[f] DRAC/SRA, Nouvelle-Aquitaine, Ministry of Culture and Communications, Poitiers, France
[g] DECOD (Ecosystem Dynamics and Sustainability), Institut Agro, INRAE, IFREMER, Rennes, France
[h] EDF R&D, LNHE (Laboratoire National d'Hydraulique et Environnement), 6 Quai Watier, Chatou Cedex, 78401, France
[i] TRACES UMR 5608, CNRS, UT2J Université de Toulouse Jean-Jaures, France
[j] Sociedad de Ciencias Aranzadi, Donostia – San Sebastián, Spain
[k] AOZTA, Bilbao, Spain
[l] Service de la conservation des musées & du patrimoine, Direction de la culture et du patrimoine, Mont-de-Marsan, France

ARTICLE INFO

Editor: H Falcon-Lang

Keywords:
Brown trout
Phenotypic variation
Upper Palaeolithic
ZooMS
Stable Isotope analysis
Sclerochronology

ABSTRACT

Human populations have relied on fish for food for thousands of years, as evidenced in numerous Palaeolithic archaeological sites across Europe. In this paper, we investigate past populations of brown trout (*Salmo trutta* L.) along the Bay of Biscay coast before, during, and after the Last Glacial Maximum and compare their phenotypic diversity with modern populations. A total of 270 salmonid vertebrae from 11 archaeological sites in Spain and France were analysed, which span c. 30 to 9 kyr cal B.P. Species identification, combining ZooMS analyses with vertebral body size, confirmed 219 specimens as brown trout, and we present a model for salmonid species identification based on vertebral size. Stable isotope analyses of carbon and nitrogen reveal a continuum of habitat use patterns. After testing multiple published regression models for body length estimation in brown trout, we develop a novel linear regression model alongside a protocol for age estimation. Overall, the analysis of body size, age and migratory ecotype demonstrates that the phenotypic diversity of brown trout populations during the Pleistocene-Holocene transition is comparable to that of modern populations, reinforcing the role of the Iberian glacial refugium in maintaining diversity during the Last Glacial Maximum. The finding of large freshwater trout alongside sea trout in human-occupied archaeological sites further suggests the exploitation of both riverine and marine fish resources by human populations.

1. Introduction

The Quaternary climatic shifts strongly affected species evolution and present ecology (Hewitt, 2000). In response to climate changes, most species relocated to more temperate, ice-free southern regions (i.e., glacial refugia [Hewitt, 2000; Kettle et al., 2011]), from which they later recolonized abandoned areas as conditions improved. The study of intraspecific variation during a glaciation-deglaciation transition provides insight into species resilience, adaptative patterns, and current distributions (Cortés-Guzmán et al., 2024; Hewitt, 2000), offering crucial information for predicting future trends under ongoing climate change (Dawson et al., 2011; Fordham et al., 2020). In this context, the

* Corresponding author at: INRAE UMR 1224 ECOBIOP, 64310, Saint Pée sur Nivelle, France.
E-mail address: ambra.d-aurelio@inrae.fr (A. D'Aurelio).

https://doi.org/10.1016/j.palaeo.2025.113073
Received 27 February 2025; Received in revised form 27 May 2025; Accepted 27 May 2025
Available online 2 June 2025

Last Glacial Maximum (LGM, 26–19 kyr B.P. [Clark et al., 2009]) represents an exceptional case study. The LGM has been widely studied, with numerous works focusing on its impact on species distribution and ecology in terrestrial organisms (e.g., Jones et al., 2020, 2021; Magri et al., 2006; Meiri et al., 2013). However, despite the significant role of aquatic resources in human subsistence and their sensitivity to climatic changes (Álvarez-Fernández, 2011; Morales-Muñiz et al., 2021; Roselló-Izquierdo et al., 2016), the impact of the LGM on aquatic ecosystems is still understudied. To this end, brown trout (*Salmo trutta* Linnaeus 1758) might be a relevant model due to its high phenotypic diversity, adaptation capacity, and potential recurrence in Palaeolithic archaeological sites. During the LGM, Spain, Portugal and southern France remained ice-free except for limited areas of mountain glaciation, making the region an important glacial refugium for many species, including fish (Kettle et al., 2011). In particular, the area was a refugium for salmonids, with numerous remains retrieved in archaeological sites in northern Spain and southern France (Adán et al., 2009; Hayden et al., 1987).

Brown trout is a diadromous fish reproducing in the headwater stretches of rivers. The migration of this species to marine habitats (anadromous ecotype) is facultative. Brown trout populations with varying proportions of anadromous and resident individuals are observed along the Atlantic coast. Brown trout alternative phenotypes result from a continuum of variation in migration patterns and phenology, including divergences in the temporal and spatial amplitudes of migration to the sea, ages at migration and diet (Etheridge et al., 2008; Ferguson et al., 2019). The migratory status and diet types result in a wide range of growth rates, size at maturation and fertility, with body size and growth rates of migratory brown trout being much higher than their resident counterparts (Ferguson, 2006). The partition into alternative life strategies, anadromous or resident, is growth-dependent and controlled by genetic and environmental factors (Acolas et al., 2012; Ferguson et al., 2019).

The growth rate of brown trout strongly depends on temperature, which modulates thus the age at migration as well (B. Jonsson and L'Abée-Lund, 1993). During the ice sheet maximum extension between 26 and 19 kyr B.P. (Clark et al., 2009), lower temperatures might have determined reduced growth rates in brown trout and, in general, lower productivity in the ecosystem. This effect was possibly higher in freshwater environments, wherein temperatures are less buffered than at sea (B. Jonsson and L'Abée-Lund, 1993; LeRoy Poff et al., 2002), making the migratory strategy more advantageous in terms of body size, growth rate, and thus fertility, at least in females. Beginning around 19 kyr B.P., with glacial ice melting, large freshwater fluxes entered surrounding oceans, gradually increasing sea levels and enhancing freshwater flow and nutrient input (Clark et al., 2009). These improved conditions might have determined higher growth rates and productivity in freshwater and marine environments, resulting in higher population densities that triggered the exploration of new environments. Long-distance dispersal of brown trout is achieved with anadromy (Elliott, 1994). Therefore, the occurence of migratory populations with large body sizes might have been crucial for post-glacial re-colonisation (Ferguson, 2006). Moreover, anadromous fish, possibly preferentially targeted by fishing activity due to their larger body size and seasonal migration, are likely more represented in ichthyo-archaeological assemblages (e.g., Halffman et al., 2015).

Most studies on Iberian archaeological salmonids focused on taxonomic identifications (Morales-Muñiz et al., 2021; Roselló-Izquierdo et al., 2016; Roselló-Izquierdo and Morales-Muñiz, 2014). Likewise, little is known about the ecology of these fish during the LGM (Morales Muñiz and Roselló-Izquierdo, 2016; Morales-Muñiz et al., 2021; Morales-Muñiz and Roselló-Izquierdo, 2008). In Asturias (NW of modern-day Spain), no significant differences in size and growth between Palaeolithic and modern salmonids were found (Turrero et al., 2012). However, the lack of discrimination between Atlantic salmon (*Salmo salar* Linnaeus 1758) and brown trout, which have different modern ecologies, weakens the conclusions of this study -an issue also underlined by Morales Muñiz et al. (2021). The body size of Palaeolithic brown trout in northern Iberia appears unaffected by temperature shifts (Blanco-Lapaz et al., 2021). Still, the species was only morphologically identified, and ecotypes were not distinguished. Despite this aspect, and the fact that multiple factors (e.g., competition for resources, selection due to the accumulator agent) might blur the results, fish fossil records have proved to be a unique palaeoecological dataset for studying ecological processes on a long-term record (Blanco-Lapaz et al., 2021). Nevertheless, they are still poorly exploited.

Species identification is a prerequisite for any study of fish ecology. Taxonomy in archaeological sites has traditionally relied on bone morphology. Though, brown trout and Atlantic salmon vertebrae morphological features are closely similar, not allowing a clear-cut distinction between the two species (Guillaud et al., 2016; Morales Muñiz et al., 2021; Watt et al., 1997). In contrast, biomolecular techniques such as DNA sequencing (Consuegra et al., 2002) and Zooarchaeology by Mass Spectrometry (ZooMS, [e.g., Korzow Richter et al., 2020]) provide reliable species identification. ZooMS relies on species-specific collagen peptides obtained from bone collagen that can remain preserved for thousands of years (Allentoft et al., 2012; Buckley and Collins, 2011; Holmes et al., 2005) and, compared to DNA sequencing, is minimally invasive and cost-effective. It is particularly effective in fish thanks to the heterotrimetry of collagen type I, meaning that, instead of the two genes that code for the collagen chains in most vertebrates, fish feature three genes (COL1A1 and COL1A2, COL1A3), increasing sequence diversity (Korzow Richter et al., 2011, 2020).

Fish body length can be inferred from vertebral size (Andrews et al., 2022; Prenda et al., 2002; Thieren et al., 2012). Bone formation occurs at different rates according to ambient water temperature, generating thin, denser (darker) winter bands and wider, less dense (lighter) summer bands (Casteel, 1976) used to estimate age in salmonid archaeological samples (e.g., Turrero et al., 2012; Blanco-Lapaz and Vergès, 2016). Age estimation combined with fork length (FL hereafter), in turn, informs about growth rates under different spatial and temporal conditions, given that growth is dependent on climatic conditions, resources, and selective pressures (Miszaniec, 2021).

The analysis of stable isotopes in bone collagen has been used to infer migratory patterns of ancient populations of salmonids (Guiry et al., 2020; Quinlan, 2023) and to study fish diet (Fuller et al., 2020; Guiry and Robson, 2024). Carbon and nitrogen stable isotope ratios differ between marine and freshwater biomes (Fry and Sherr, 1984; Owens, 1985), offering the opportunity to infer anadromy in fish populations (Charles et al., 2004). Notably, the bone collagen of an anadromous trout that feeds on marine prey is ^{13}C-enriched compared to a resident trout feeding on freshwater prey (Goodwin et al., 2016; Ruokonen et al., 2019), enabling the study of habitat use tactics through carbon stable isotope analysis akin to studies of habitat shifts in terrestrial animals in response to environmental change (e.g., Jones et al., 2020, 2021).

The present work aims to study the body length, age and migratory ecotype of *S. trutta* during the Pleistocene-Holocene climatic transition to assess the impact of climatic changes on intraspecific diversity when human impact was relatively low. The study presented in this paper targeted the Iberian glacial refugium and its northern margins (i.e., up north to the Loire River), which is one of the main glacial refugia during the LGM, thought to have been central in the northward post-glacial recolonization of brown trout (e.g., Cortey et al., 2009).

We expect that growth rates of brown trout were lower during the coldest periods of the Pleistocene-Holocene transition than during the warmer periods. A gradient of growth rate values between the core of the Iberian glacial refugium (warmer area) and the northern margin of the refugium is also expected. The fact that all the current brown trout populations along the Atlantic coast bear a high diversity of life history suggests that this overall strategy provides an evolutive advantage. Therefore, we also wanted to test whether this diversity was conserved over time and if migratory and resident ecotypes of brown trout were observed together during the Pleistocene-Holocene transition.

The investigation was undertaken by combining multiple approaches applied together for the first time to Palaeolithic salmonid remains. These include ZooMS, bone collagen isotopic composition, bone morphometry, sclerochronology to infer species, ecotype, diet, body length, age and growth.

2. Materials and methods

2.1. Study sites and sample selection

Trout vertebrae come from 11 archaeological sites, all karstic caves (except the Duruthy rock shelter) located in the Cantabrian region of the Iberian glacial refugium and its northern (French) margins, occupied by hunter-gatherers during the targeted period (Table 1 and Fig. 1). Sites occupations dated between the mid-final Upper Palaeolithic (c. 30 to c. 9 kyr cal B.P.), spanning the Gravettian, Solutrean, Magdalenian and Azilian cultural periods (Table 1), a timespan marked by significant climatic fluctuations (brief descriptions of the archaeological sites are in Supplementary File A). Most specimens were initially identified as *S. trutta* based on a morphological classification system that categorizes vertebrae by their vertebral body shape and the feature and density of the lateral pores (Guillaud et al., 2016; Le Gall, 1984). Vertebral size was excluded as an identification criterion to avoid the potential elimination of large anadromous brown trout. A total of 270 vertebrae identified as *Salmo* spp. (of which 33 morphologically identified as *S. salar* and 155 as *S. trutta*, example of brown trout vertebra in Fig. 2a) were selected. The vertebrae likely belonged to different individuals as samples came from different square meters and layers within the excavations, and vertebrae varied substantially in their dimensions. Species identification was subsequently confirmed, or infirmed, through ZooMS, based on collagen type I sequencing. Collagen extraction for carbon and nitrogen stable isotope analysis (SIA) was performed on 153 samples, and a subset of 144 bones were subjected to ZooMS analyses. Selection for SIA and ZooMS analysis was based on the amount of available bone material and, in the case of ZooMS, on collagen preservation (Fig. 3). FL was estimated on all 270 samples, while age was inferred on that subset of 219 vertebrae identified as brown trout. A table resuming the information about each sample and the analysis carried out is available as Supplementary Table S1.

2.2. Collagen extraction

Of the 270 samples, 153 salmonid vertebrae recovered from levels dated from 30 to 9 kyr B.P., and 15 contemporary trout (6 anadromous and 9 resident trout) from 6 sites in southern France (details on the reference modern dataset can be found in Supplementary File B) were processed for collagen extraction in the EvoAdapta lab facilities at the University of Cantabria (Santander, Spain). Bone samples (at least 20 mg each) underwent collagen extraction using established protocols (Matsubayashi et al., 2017; Mion et al., 2022). Archaeological bones were cleaned, measured, and photographed before destruction. Bones weighing less than 100 mg were demineralized with 0.1 M HCl, whereas those over 100 mg were demineralized with 0.5 M HCl, with daily acid changes until demineralization was completed. Samples were then rinsed five times with distilled water, soaked in 0.125 M NaOH for 30 min at room temperature, and rinsed again. Gelatinization was conducted at pH 3 for 48 h at 75 °C. The resulting samples were filtered with Ezee filters (selectivity: 60 to 90 μm) and decanted into duplicate tubes sealed with parafilm, frozen for 48 h, and lyophilized for 1–2 days, following the protocol by Mion et al. (2022) modified from Cersoy et al. (2017). The 15 samples of contemporary vertebrae (Supplementary Table S2) were processed using the protocol by Matsubayashi et al. (2017), modified from Longin (1971), which includes a degreasing step (6 h in 1:1 methanol:chloroform solution, followed by two rinses with 99.5 % methanol and five washes with distilled water) before demineralization. Archaeological samples were not subjected to degreasing, as we assumed that taphonomic processes had already reduced their lipid content below 5 % of the bone weight, a threshold above which lipids might significantly affect isotopic values (Guiry, Szpak, et al., 2016). On 6 contemporary sea trout, the centre of the vertebral bodies, representing the juvenile stage featuring the freshwater signature, was isolated from the peripheral portion (i.e., the adult life stage), which, in migratory fish, incorporates the seawater signature (Fig. 2b). Collagen extraction was conducted separately on each portion. This approach could not be applied to the archaeological vertebrae due to their friability and poor organic matter preservation.

Of the 153 archaeological specimens processed through the Mion et al. (2022) protocol, collagen of 39 samples was used for ZooMS analysis. For 105 samples (of which 90 did not yield sufficient collagen following the Mion et al. (2022) protocol, and 15 that were not selected for the isotopic stable isotope analysis) collagen extraction was repeated to perform ZooMS analysis (Fig. 3). The ammonium bicarbonate (AmBic) method (Section 2.3), adapted for bone samples as small as 10 mg (van Doorn et al., 2011), was employed, as ZooMS requires only a few milligrams of collagen.

2.3. Species identification through ZooMS analysis and vertebrae morphometry

A total of 144 archaeological specimens were submitted to ZooMS analysis for species identification. Samples consist of collagen previously extracted (39 samples) or vertebrae fragments (105 samples, average weight ± 12 mg). Samples selection was based on the availability of either collagen extracted for the SIA analysis or osseous material (Fig. 3).

ZooMS is a minimally destructive method for taxonomic identification based on collagen peptide mass fingerprinting (Buckley et al., 2009). The extraction and digestion of collagen type I followed published protocols (Buckley et al., 2009; Welker et al., 2015) and was obtained using the AmBic technique (van Doorn et al., 2011) in the lab facilities of the EvoAdapta group in the University of Cantabria. All 105 bone samples (~6–30 mg) were incubated in 100 μl of 50 mM ammonium-bicarbonate (NH3CO3, AmBic) buffer at 65 °C for one hour. After that, the samples were demineralized in 150 μl of 0.6 M hydrochloric acid (HCL) at 4 °C. After neutralization with 50 mM ammonium-

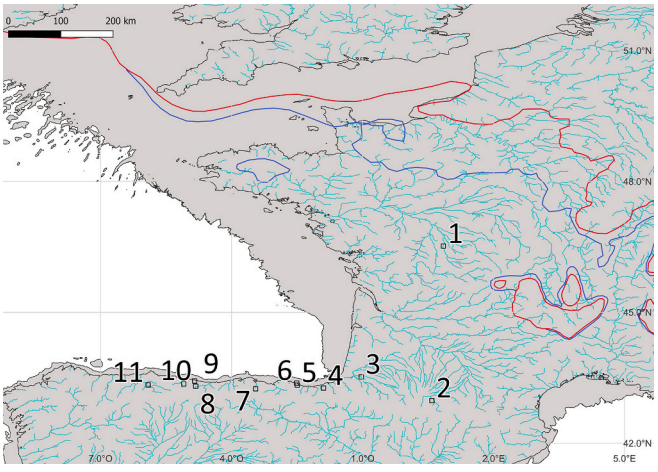

Fig. 1. Geographical distribution of the archaeological sites. Geographical distribution of the eleven archaeological sites included in the study: 1. Taillis Des Coteaux, 2. Troubat, 3. Duruthy, 4. Aitzbitarte III, 5. Laminak II, 6. Santa Catalina, 7. El Mirón, 8. Los Canes, 9. La Riera, 10. El Buxu, 11. Las Caldas. The grey shading represents the coastline during the Last Glacial Maximum (LGM), while the blue and red lines indicate the extent of the discontinuous/sporadic permafrost and continuous permafrost during the LGM, respectively (Lambeck et al., 2014; Opel et al., 2024; Stadelmaier et al., 2021). (For interpretation of the references to colour in this figure legend, the reader is referred to the web version of this article.)

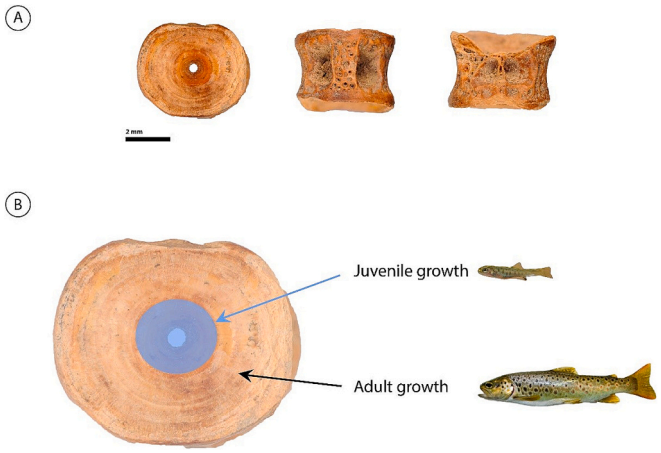

Fig. 2. Vertebrae of brown trout. (A) Archaeological vertebrae of a brown trout from the archaeological site of El Mirón: transversal, dorsal and ventral view of the vertebral body. (B) Sampling strategy adopted for stable isotope analysis (SIA) on six contemporary anadromous brown trout vertebrae: juvenile (in blue in the figure) and adult portions were physically separated and analysed independently. (For interpretation of the references to colour in this figure legend, the reader is referred to the web version of this article.)

bicarbonate (NH3CO3, AmBic), all 144 collagen samples were incubated in 100 µl of AmBic at 65 °C for 1 h. Then, 50 µl of the resulting supernatant was digested using trypsin (0.5 µg/µl, Promega) between 12 and 18 h at 37 °C, acidified by adding 1 µl of 10 % trifluoroacetic acid and cleaned on C18 ZipTips (Thermo Scientific).

Collagen-digested peptides were then spotted in triplicates on a MALDI Bruker plate, adding αCyano-4-hydroxycinnamic acid as a matrix. MALDI-TOF MS analysis was performed at the University of York (UK) on a Bruker UltrafleXtreme with a mass range of 800–4000 Da.

Spectral triplicates for each sample were merged using R v.4.2.3 (R Core Team, 2023) using the MALDIquant package (Gibb and Strimmer, 2012), obtaining .msd files. Taxonomic identification was made manually in MMass v. 5.5.0 (Strohalm, 2023). The table of *m/z* values was then compared with a reference library of acknowledged peptide markers (Buckley et al., 2022; Harvey et al., 2018; Korzow Richter et al., 2020).

Among the diagnostic peaks for Salmonids, some are specific to *S. trutta* or *S. salar*, allowing species discrimination. The peptide position COL1α3 568–579 is considered the most reliable marker (Quinlan, 2023), with *S. salar* showing an m/z peak of 1026 and *S. trutta* displaying an m/z peak of 996 (Harvey et al., 2018; Buckley et al., 2022; Quinlan, 2023, Fig. 4).

To complement species identification based on morphological criteria on those samples that remained undetermined through ZooMS,

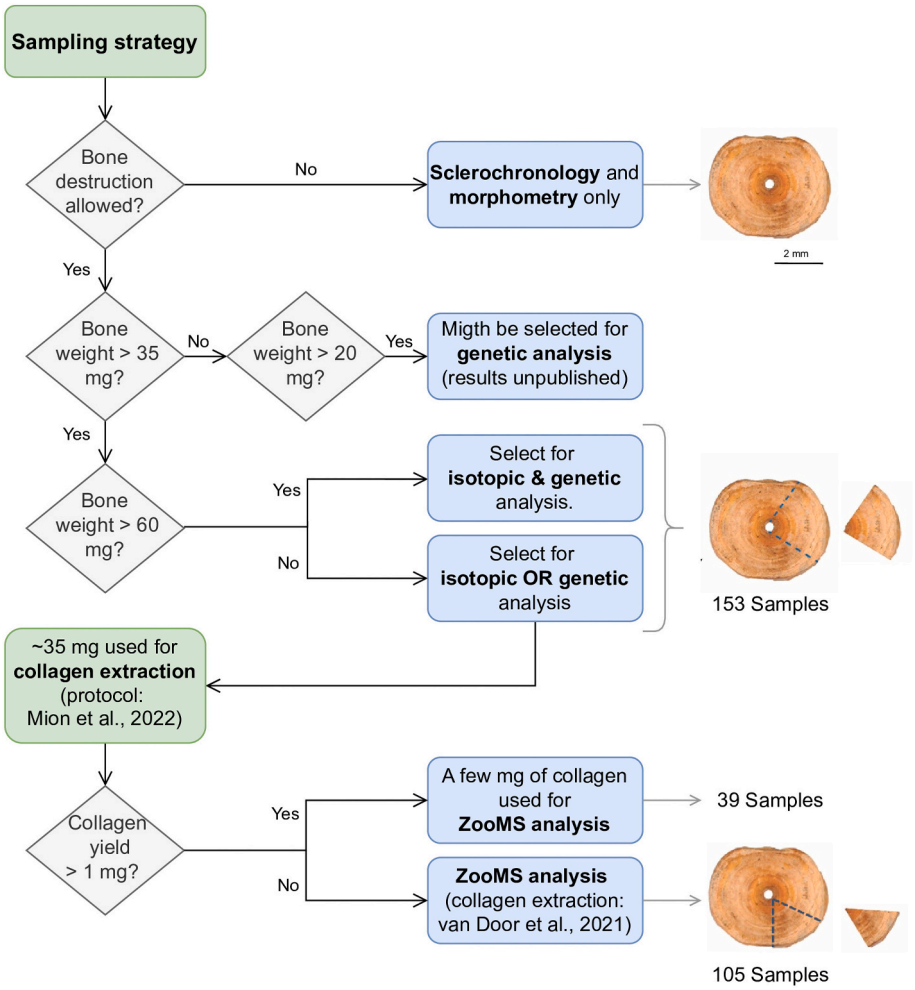

Fig. 3. Sampling strategy. The flowchart shows the sampling strategy used in this work, which is based mainly on the amount of available bone material. A portion of at least 35 mg of vertebral bone was used for collagen extraction for δ13C and δ15N stable isotope analysis (SIA) for 153 archaeological vertebrae through the protocol by (Mion et al., 2022). A few mg of the obtained collagen was used for ZooMS analysis for 39 samples. On an additional 105 samples, a further fragment of bone of ~10 mg was used for collagen extraction for ZooMS analysis through the protocol by (van Doorn et al., 2011).

Table 1
Geographical and temporal distribution of the 270 selected archaeological specimens of salmonids. GRAV., SOL., LM, MM, UM and AZ stand for Gravettian, Solutrean, Lower Magdalenian, Middle Magdalenian, Upper Magdalenian and Azilian cultural periods, respectively. LGM stands for Last Glacial Maximum.

Site		Department/Province	GRAV.	SOL.	LM	MM	UM	AZ	
			Pre-LGM	LGM		Post-LGM	Yonger Dryas (YD)	Post-YD	Sample size
			~30–21 kyr B.P.	~21–18 kyr B.P.	~18–11 kyr B.P.			~11–9 kyr B.P.	
1	Taillis des Coteaux	Vienne	26		31	6			63
2	Troubat	Haute-Pyrénées					14	4	18
3	Duruthy	Landes				2			2
4	Aitzbitarte III	Gipuzkoa	6						6
5	Laminak II	Bizkaia					16	6	22
6	Santa Catalina			2		25	11	5	43
7	El Miron	Cantabria		10	15	11	5	2	43
8	Los Canes				6		8	10	24
9	La Riera	Asturias		10		2			12
10	El Buxu			6					6
11	Las Caldas			6		17	8		31
			32	34	52	63	62	27	270

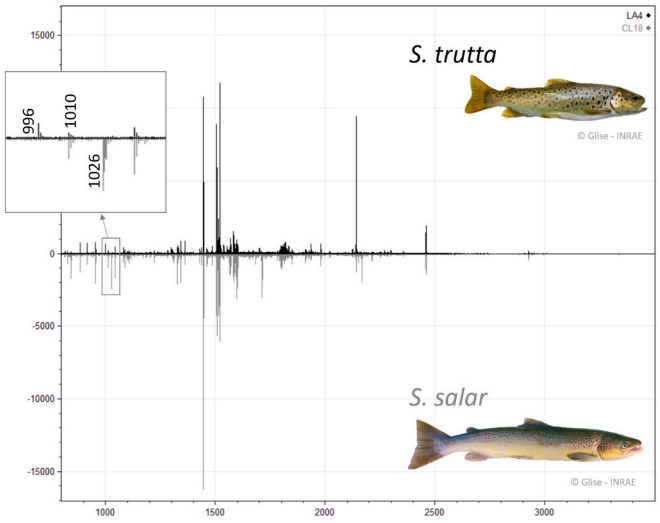

Fig. 4. *S. salar* and *S. trutta* ZooMS major diagnostic peaks in MALDI-TOF spectra. The peptides of collagen type I of two Salmonids analysed in the present study are shown in the picture as they appear in the MMass software: the peaks of a brown trout sample from Laminak II in black and an Atlantic salmon from Las Caldas in grey. (For interpretation of the references to colour in this figure legend, the reader is referred to the web version of this article.)

we developed a linear regression model based on the vertebral size of the vertebrae identified through ZooMS.

Previous studies indicated different criteria to distinguish the two species. The vertebrae size is one of these, although it might lead to the mis-assignment of anadromous brown trout as Atlantic salmon (Guillaud et al., 2016). The vertebral body shape and lateral pores shape and distribution have also been indicated as possible criteria for species identification (Guillaud et al., 2016; Le Gall, 1984). We checked whether a significant difference between vertebral height (M1), width (M2), and length (M3) of *S. trutta* and *S. salar* exists (Supplementary File C) and, through the Fisher's exact test, tested the correlation between ZooMS-assigned species and: i) the ratio between M1 and M2, as brown trout vertebrae shape seems more elliptical (M1/M2 < 1) than in Atlantic salmon (Guillaud et al., 2016); ii) vertebral body shape, assigning it to brown trout when elliptical and to Atlantic salmon when rounded; iii) the lateral pores shape of the vertebra, assigning brown trout when pores shape was more elongated, their size homogenous within the same vertebrae and the disposition regular, and as Atlantic salmon when their shape was more rounded, the size variable and the distribution irregular as observed in the contemporary skeletons.

We generated a binomial generalised linear regression per each vertebra measure -with the probability threshold for species identification set to 0.95- and used ZooMS-identified samples to calculate the model prediction error. The species was assigned if the results obtained from different measurements of the same vertebra (i.e., M1, M2, or M3) were in accordance. Specimens with a FL < 23 cm were not identified as they might be pre-smolts of Atlantic salmon. Indeed, it seems reasonable, according to data found in the literature (Gregory et al., 2018; N. Jonsson and Jonsson, 2007; Letcher and Gries, 2003; Økland et al., 1993; Saloniemi et al., 2004), that Atlantic salmon with body length longer than the chosen conventional threshold of 23 cm already migrated to the sea.

2.4. Carbon and nitrogen stable isotope analysis (SIA)

The ecotype and trophic behaviour of past brown trout were investigated using stable isotopes analysis (SIA) of collagen carbon and nitrogen. Collagen was extracted from 153 archaeological specimens and 15 modern specimens (for reference) following the protocol by (Mion et al., 2022, see section 2.2). Archaeological samples were selected based on their weight and to ensure a spatiotemporal stratification of the data points (Fig. 3). Carbon and nitrogen contents and isotope composition (δ^{13}C and δ^{15}N), were measured by placing tin capsules containing dry material into an elemental analyser (vario ISOTOPE cube, Elementar, Langenselbold, Germany). The analyser was coupled, via a gas box interface, to a continuous-flow isotope ratio mass spectrometer (Isoprime100, IRMS, Elementar UK, Cheadle, United Kingdom) available at SILVATECH (SILVATECH, 2018). 10.15454/1.5572400113627854E12 Elementary gases were analysed by isotope ratio mass spectrometry using Isoprime100 IRMS (Cheadle, United Kingdom). Carbon and nitrogen contents were expressed as a percentage of dry matter, while stable isotope values were expressed as delta values (δ^{13}C and δ^{15}N, in ‰) relative to the Vienna Pee Dee Belemnite (V-PDB) standard for C and air N2 for N. The δ^{13}C uncertainty of measurements is 0.3 ‰ (2σ), while it is 0.5 ‰ (2σ) in nitrogen.

Collagen quality was assessed using the carbon-to-nitrogen atomic ratio (C:N atomic), which helps identify contamination from exogenous carbon or nitrogen (Ambrose, 1990; DeNiro, 1985). For archaeological samples, the traditional (DeNiro, 1985 [range: 2.9–3.6]) and revised standards for archaeological fish, especially valuable for δ^{13}C contamination (Guiry and Szpak, 2021 [range varies according to δ^{13}C value]), were applied to interpret C:N. In the latter case, we considered cold-water fish (CWF) liberal ranges, assuring a deviation in δ^{13}C of < -1.0 ‰. The standards proposed for modern fish (Guiry & Szpak, 2020 [range 3.00-3.30]) were applied to the contemporary samples.

2.5. Ecotype assignment through supervised and unsupervised models

Ecotype classification of archaeological samples was achieved using two approaches: a non-supervised classification based solely on stable isotope data from archaeological specimens and a supervised classification using stable isotope values from modern brown trout with known ecotypes.

Hierarchical clustering was applied as a non-supervised classification to archaeological samples, using $\delta^{13}C$, $\delta^{15}N$, FL and vertebral dimensions as explanatory variables. Different combinations of these variables were tested in clustering models implemented in R (using the R *cluster* package), with the number of clusters (k) ranging between 2 and 15 for each combination. The model with the highest Silhouette index was selected for final classification. For the supervised classification, we compiled a dataset of $\delta^{13}C$ and $\delta^{15}N$ values from 114 modern brown trout specimens (41 anadromous and 73 resident), including 59 published and unpublished data points from north-western France (latitude $\sim +48°N$, (Charles et al., 2004; this data were corrected for lipid bias as suggested by Post et al. [2007]), 49 published from northern Finland (latitude $\sim +70°N$, Ruokonen et al., 2019) and 6 from southwestern France (latitude $\sim +43°N$, this study). For modern values obtained from fin or muscle tissues, a $\delta^{13}C$ correction of +3.69 was applied (Guiry et al., 2020) to account for tissue-specific isotopic differences. A Suess effect correction was also applied to modern samples using different correction factors for freshwater and marine environments as the depletion of heavy carbon due to anthropogenic activities differs in these environments (Guiry et al., 2020). Freshwater values correction followed the equation from Verburg (2007). For the marine environment correction equation (Guiry et al., 2020), we applied an annual rate of $\delta^{13}C$ decrease for water body (i.e., North Atlantic Ocean) of −0.024 (Quay et al., 2007), and the shape of the exponential curve defined by a decrease in oceanic $\delta^{13}C$ of 0.027 (Gruber et al., 1999; Guiry et al., 2020). The corrected $\delta^{13}C$ values were significantly different between anadromous and resident ecotypes, which was the basis of the ecotype classification. A bootstrapped (1000 iterations) generalised linear model (GLM) with a logistic link function was based on the $\delta^{13}C$ values. Incorporating data from different latitudes allowed the model to mitigate the latitude effect. The model predicted the probability of an individual being anadromous based on its $\delta^{13}C$ value:

$$P_{(\text{ecotype}=\text{“anadromous”})} = 1 \div \left(1 + e^{-(37.700375 + 2.207648^{*}\ \delta 13C)}\right) \quad (1)$$

A probability threshold of 0.80 was used for ecotype assignment. The error rate of the model, calculated using the 114 specimens of the modern database with known ecotypes, is 0.026 (false resident rate: 0; false anadromous rate = 0.026). The model "undetermined" fish ($P < 0.80$ for both resident and anadromous classification) rate is 0.079, of which 78 % were anadromous and 22 % were resident. Supervised and unsupervised classifications were combined: samples classified identically by both methods were deemed conclusive, whereas discordant classifications were noted as “undetermined”.

2.6. Fork length, age and growth rate estimation

We inferred ancient brown trout FL, age, and growth rate (GR hereafter) through allometric and sclerochronological analyses.

FL is one of the alternative measures of fish body size, together with the total and standard length. FL (distance from the tip of the longest jaw to the centre of the fork in the caudal fin [Kahn et al., 2004; Miller and Robert, 1972]), was selected because its measurement method is more precise and, compared to the total length, has a higher correlation with the vertebral column length, as it does not depend on the caudal lobes dimension.

To develop accurate references for FL and age estimation, we assembled a reference collection of 52 modern brown trout from different ecotypes and life stages, sampled from various regions along the Atlantic coast (Hereafter dataset S3. Details on this dataset are in Supplementary File B and Supplementary Table S3). Sampling was stratified according to age (0–9 years), FL (8–76 cm), and sex. Age was estimated through scalimetry following Baglinière et al. (2020). M1, M2 and M3 were measured on each vertebral centrum following Morales Muniz and Rosenlund (1979). Based on FL and vertebral dimensions of 49 modern brown trout specimens from dataset S3, we developed allometric models per each vertebral dimension and vertebra type identifiable along the vertebral column: (a) the atlas; (b) vertebrae without fused neural/haemal spinous processes (NS); and (c) vertebrae with fused neural/haemal spinous processes (S). A fourth group, the vertebrae of the urophore complex (i.e., the last three elements of the vertebral column), was excluded from FL estimation due to the high variability of measurements among these three vertebrae. Vertebral dimensions of samples in dataset S3 are available in Supplementary Table S4. Two 0+ samples -SK70 and SK71- were not used for the allometric regression as the vertebrae were too small to be precisely measured. As incomplete preservation due to mechanical and chemical damage often limited the measurable dimensions of archaeological vertebrae to one or two instead of all three, we generated individual allometric equations for each dimension instead of combining them into a single regression model.

Within the NS and S groups, the precise position of an archaeological vertebra within the column is impossible to determine, as these cannot be placed in order within each group (Morales, 1984). Hence, in these two cases, all specimens from the same category were pooled together when calibrating the body-vertebrae regressions. To this end, we tested different modelling approaches: i) a bootstrapping approach with 1000 iterations versus the use of the mean dimension per group; ii) the use of the whole set of fish versus using fish with FL > 30; iii) linear versus exponential models; and selected the best according to R-squared, which indicates the proportion of variance in the dependent variable explained by the model. For the atlas, a linear regression model per each dimension was generated. Among the selected models per each vertebrae type and measure, we predicted FL on archaeological vertebrae by applying the most accurate model considering the available measurements for each sample. Previously published models were not adequate for this study since some were not only based on both *S. trutta* and *S. salar* modern samples but also more restricted in terms of vertebral categories (Feltham and Marquiss, 1989; Prenda et al., 2002; Van Neer et al., 1999), measurements (Feltham and Marquiss, 1989; Le Gall, 1984; Prenda et al., 2002; Turrero et al., 2014; Van Neer et al., 1999), and range of body sizes and/or life stages considered (Feltham and Marquiss, 1989; Van Neer et al., 1999). Nonetheless, the regression models from these publications have been tested on dataset S3.

The ensemble of the analyses is available in Supplementary File D.

Age was estimated using sclerochronology. At least one vertebra for each contemporary fish in dataset S3 was photographed with a binocular stereomicroscope using the cellSens Imaging software, with a 1× objective and magnification ranging from 0.5 to 10. Multiple images of each archaeological vertebra were taken with an APN Nikon D300s camera and Nikon AF-S VR105 mm lens at different focal depths and combined using Combine ZP software, providing detailed views of each vertebra. As, unlike scalimetry, age estimation from vertebrae is not a standard method in ecological studies of *S. trutta*, and, to the best of our knowledge, no formal protocols are available, we first established a protocol for age estimation by examining 24 modern specimens (hereafter training set) with known ecotypes (previously determined from scales), and, then assessed its accuracy by estimating the age of 28 additional specimens (hereafter validation set) without consulting their known scale-derived ages. Two readers were involved, one of whom was an expert in reading salmonid scales (hereafter expert reader) and the other without previous experience in sclerochronology (hereafter candid reader). Dataset S3 was partitioned into a training and a validation set (see Supplementary Table S3). Age was estimated by counting annuli in vertebral images in Otolithe (https://github.com/inrae/otolithe), an

application developed to facilitate collaborative sclerochronological analyses. Special attention was given to the vertebral pattern and dimensions of juveniles (0+ and 1+) to help interpret the first year of life, one of the most challenging phases. The training phase provided a protocol for vertebral annuli counts (Supplementary File E). After the validation phase, vertebra- and scale-derived ages were compared and precision (i.e., variation among operators' estimates) and accuracy (difference between scale-derived and vertebra-derived ages) were calculated for each modern vertebra using, respectively, the coefficient of variation (CV, Vitale et al., 2019) and the mean absolute error (MAE, Hodson, 2022).

The two readers applied the validated protocol to the archaeological vertebrae. In this case, only the coefficient of variation was calculated to assess precision. Finally, an average, maximum and minimum age were assigned to each vertebra considering the estimates of the two readers. Maximum and minimum GRs were calculated by dividing maximum and minimum FL for minimum and maximum age.

2.7. Statistical analyses

All statistical analyses were performed using R (version 4.2.3, R Core Team, 2023). The object of this analysis was two-fold. First, we investigated significant differences in FL, age and GR correlated to ecotypes, nitrogen signatures, periods, and geographical areas. Second, we assessed the effect of spatiotemporal variation on ecotype and nitrogen signatures. Climatic conditions were also considered. The dating of the major climatic events of the studied period and correspondence with the study samples is based on the integration of ice cores and marine and terrestrial records (Rasmussen et al., 2014), as illustrated in Table 2.

Non-parametric tests were used in this study as the data did not fulfil the conditions for parametric tests; Spearman's test was used to test the correlation between two continuous variables; Wilcox's test tested the effect of a categorical binomial variable on a continuous one, Kruskal-Wallis' test tested the effect of a categorical variable with more than two conditions on a continuous one, and Scheirer-Ray-Hare's test, tested the effect of two categorical variables on a continuous one.

3. Results

3.1. Taxonomic identification

Among the 270 archaeological salmonid samples pre-selected through morphological criteria, collagen spectra generated in 144 via ZooMS allowed species identification of 99 samples (69 %). Of these, 72 (73 %) were identified as *S. trutta,* and 27 (27 %) as *S. salar* (Supplementary Table S6). Due to poor preservation, one-third of the analysed specimens (45 samples) produced incomplete type I collagen spectra, precluding species-level identification. In some cases, unresolved samples exhibited mixed peaks consistent with multiple fish species, including *S. salar* and *S. trutta*. These 45 unidentified samples and 126 not analysed with ZooMS left 171 specimens unidentified biomolecularly.

The combination of ZooMS analysis and vertebral measurements revealed significant differences in the sizes of *S. salar* and *S. trutta* vertebrae for all three measurements (M1, M2, M3, Wilcox test *p*-value = 6.45e-12 to 0.0044, see Supplementary File C), despite a partial overlap of the range, which is reduced when the S and NS vertebrae groups are considered individually (Supplementary Table S7). The range of measurements in *S. trutta* and *S. salar* are reported in Supplementary Table S7 and displayed in Fig. 5. Pores and body shape observation resulted to be correlated with the species only in the NS vertebrae type (Fisher's exact test p-value: 1.16e-05 for pores and 0.037 for body shape). On the contrary, in our dataset, the M1:M2 ratio is not significantly different in the two species. Hence, these results suggested vertebral size as a tool to discriminate species in 171 unidentified samples. A binomial logistic regression model was applied to this end based on vertebral size range thresholds determined from ZooMS spectra (Supplementary File C). Ultimately, 219 of the initial 270 vertebrae were identified as brown trout (see Supplementary Table S1).

3.2. Stable isotopes analysis: quality control

Of the 153 ancient samples subjected to collagen extraction, 129 (84 %) yielded collagen. Carbon and nitrogen stable isotope ratios were successfully measured in 77 samples (59 % of the analysed sample), while for 52 samples, the concentration of the elements did not reach the instrument detection limit. Among the 77 measured samples, 37 (48 %) met the quality criteria from DeNiro (1985). 26 out of 37 were identified as *S. trutta* (Table 3) and 11 as *S. salar* via either ZooMS or the binomial logistic regression model for species identification presented in section 3.1. 30 samples, of which 21 (one additional and six less compared to the traditional criteria) brown trout and 9 Atlantic salmon passed the revised quality criteria (Guiry and Szpak, 2021). The ensemble of the results is reported in Supplementary Table S1. The SIA results presented in this work concern the 37 samples that fit into DeNiro (1985) criteria. However, the $\delta^{13}C$ values of the six excluded brown trout following Guiry and Szpak (2021) are indicated in Table 3 through an asterisk and might be interpreted cautiously. $\delta^{13}C$ vs C:N ratio is displayed in Supplementary Fig. S1.

4 out of 15 modern samples here analysed did not meet the quality criteria (Supplementary Table S2).

3.3. $\delta^{13}C$ and ecotype assignment

Hierarchical clustering analysis on the 37 archaeological samples revealed that the optimal clustering model used $\delta^{13}C$ alone with a cluster number (k) of 2. The output of this model, combined with the probability calculated by Eq. 1 revealed a large diversity of migratory tactics (Figs. 6 and 7a, Table 3), as 6 (23 %) brown trout samples were classified as resident ($\delta^{13}C$ range: −24.7 ‰ to −19.8 ‰), 7 (27 %) as anadromous ($\delta^{13}C$ range: −16.2 ‰ to −12.3 ‰), and the remaining 13 (50 %) exhibited intermediate signatures ($\delta^{13}C$ range: −18.6 ‰ to −16.5 ‰).

Table 2
Climatic events occurred during the studied period. The cultural periods of the samples and related dating are reported here, together with the corresponding glaciation phase and climatic events and their chronology, according to Rasmussen et al. (2014). GS and GI stand for "Greenland stadial" and "Greenland interstadial", representing colder and warmer phases of the North Atlantic region, respectively.

Cultural period	Dating (kyr B.P.)	Glaciation phase	Climatic event	Climatic condition	GS/I dating (kyr B.P.)
Azilian	11–9	interglacial	Holocene interglacial period	warm	<11.7
Upper Magdalenian	13–11	deglaciation	GS-1	cold	12.9–11.7
Magdalenian	18–13	deglaciation	GI-1	warm	17.5–12.9
Solutrean	21–18	LGM	GS-2	cold	23.2–17.5
Upper Gravettian	26–21	LGM	GS-3	cold	27.5–23.3
Gravettian	> 26	pre-LGM	GS-4	cold	28.6–27.8
Gravettian	> 26	pre-LGM	GS-5	cold	32.0–28.9
Gravettian	> 26	pre-LGM	GS-6	cold	33.4–32.5

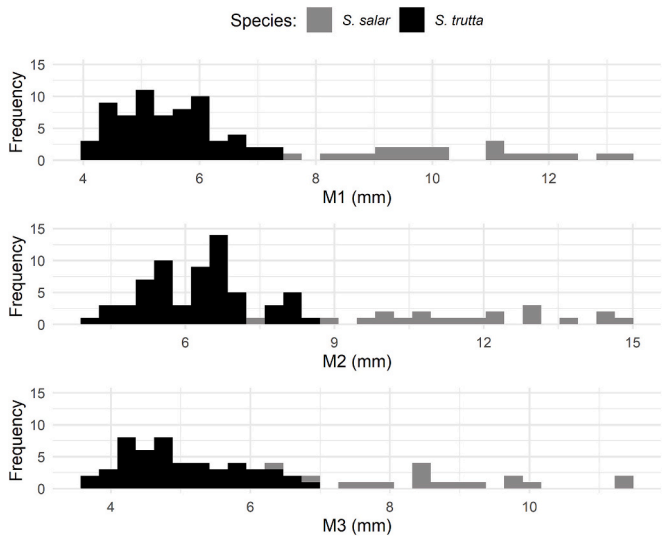

Fig. 5. Vertebrae dimensions of brown trout ($n = 72$) and Atlantic salmon ($n = 27$). M1, M2 and M3 of vertebrae identified through ZooMS are displayed for the ensemble of the vertebrae (type S and NS). The distributions are differential in the two species and only partially overlapping.

Among the 11 *S. salar* samples, 6 were classified as anadromous, 2 as resident, and 3 remained undetermined.

3.4. $\delta^{15}N$ in different environments

$\delta^{15}N$ values ($n = 26$) were significantly different between marine and freshwater environments (Kruskal-Wallis test, p-value = 0.0084. Dunn test: resident-anadromous p-value = 0.0033; anadromous-undetermined, p-value = 0.28; resident-undetermined, p = 0.0413) and ranged between 5.54 ‰ to 9.14 ‰ in resident fish, 6.08 ‰ to 13.6 ‰ in undetermined fish and 8.66 ‰ to 16.0 ‰ in anadromous fish (Table 3, Fig. 7a and Supplementary Fig. S2). A positive significant correlation between $\delta^{15}N$ and $\delta^{13}C$ values was also observed (Spearman test, p-value = 0.00027).

Using a Gaussian Mixture Model (GMM) implemented with the *Mclust* R package, $\delta^{15}N$ distributions were analysed for each ecotype. For anadromous trout, the model identified two components (BIC = −35.0) with mean $\delta^{15}N$ values of 9.2 ‰ ± 0.13, 14 ‰ ± 1.67. In contrast, resident and undetermined trout exhibited unimodal distributions with mean $\delta^{15}N$ values of 7.6 ‰ ± 1.43 (BIC = −22.7) and 10.0 ‰ ± 4.52 (BIC = −61.6), respectively.

3.5. $\delta^{13}C$ and $\delta^{15}N$ on modern samples

The $\delta^{13}C$ and $\delta^{15}N$ values of 12 modern anadromous and resident trout analysed for this study ranged between −20.2 ‰ and − 11.1 ‰ ($\delta^{13}C$ values corrected for tissue-related and Suess effect) and from 10.5 ‰ to 13.3 ‰ ($\delta^{15}N$ values). The results are available in the Supplementary Table S8. The average $\delta^{13}C$ values for the external portion of anadromous trout vertebrae (n = 5), central portion of anadromous trout vertebrae ($n = 3$), and resident trout vertebrae ($n = 6$) were − 11.6 ‰ ± 0.30, −14.6 ‰ ± 0.82, and − 17.4 ‰ ± 2.19, respectively (Supplementary Fig. S3). $\delta^{13}C$ values significantly differed between external portion of anadromous trout vertebrae and resident trout vertebra only (Dunn test p-value = 0.0038). The Dunn test p-value for the comparisons "anadromous trout adult stage – anadromous trout juvenile stage" (Fig. 2b) and "anadromous trout juvenile stage – resident trout" was 0.38 and 0.71, respectively. Average $\delta^{15}N$ values were 13.0 ‰ ± 0.30 for the external portion of anadromous trout vertebrae, 11.6 ‰ ± 0.85 for

Table 3
Stable isotope analysis (SIA) results and assigned ecotype of brown trout archaeological samples from this study, for which migratory patterns were studied based on $\delta^{13}C$ values. Information on the archaeological site, cultural period, climatic phase, estimated fork length ± RSE (residual standard error), estimated age (candid vs expert), and average growth rate are also included. The reported data concerns the samples that fit the quality criteria by DeNiro (1985), using one decimal. The asterisks display the samples excluded according to the cold-water (CWF)-liberal range from Guiry and Szpak (2021).

Site		ID	Cultural period	Climatic phase	Vertebra type	FL (cm)	SRE (cm)	Age (candid)	Age (expert)	Average growth rate	$\delta^{15}N$ (‰)	$\delta^{13}C$ (‰)	Ecotype
1	Taillis Des Coteaux	TC52	MM	GI-1	NS	46	3	3	2	18.38	9.43	−14.38	anadromous
		TC50	MM	GI-1	S	47	4	3	2	18.73	9.78	−16.54	undetermined
		TC33*	LM	LGM	NS	41	3	4	6	8.26	9.41	−14.74	anadromous
		TC54	LM	LGM	S	46	4	4	4	11.45	8.66	−14.80	anadromous
		TC56*	LM	LGM	S	40	4	2	2	20.04	7.88	−16.75	undetermined
		TC34	LM	LGM	NS	43	3	3	5	10.69	8.23	−17.45	undetermined
		TC37*	LM	LGM	NS	45	3	3	4	12.73	10.02	−17.16	undetermined
2	Troubat	MB10	Early Holocene	Holocene interstadial	NS	44	3	–	–	–	16.01	−12.30	anadromous
		MB18	UM	GS-1	NS	46	3	3	–	15.37	13.46	−15.57	anadromous
		MB14	UM	GS-1	S	56	4	3	2	22.32	12.49	−16.17	anadromous
		MB11	UM	GS-1	NS	48	3	–	–	–	8.51	−19.83	resident
		MB12	UM	GS-1	NS	43	3	–	–	–	8.21	−19.94	resident
5	Laminak II	LA18	AZ	Holocene interstadial	NS	48	3	3	5	12.07	6.76	−21.02	resident
		LA4	UM	GS-1	NS	56	4	5	4	12.50	13.91	−15.60	anadromous
		LA16	UM	GS-1	NS	47	3	3	2	18.63	13.60	−16.65	undetermined
		LA1	UM	GS-1	NS	50	3	4	3	14.40	12.70	−17.16	undetermined
		LA6	UM	GS-1	NS	49	3	2	3	19.47	12.07	−18.03	undetermined
7	El Miron	MR41*	AZ	Holocene interstadial	NS	38	3	2	2	18.82	9.18	−17.72	undetermined
		MR1*	Solutrean	LGM	NS	50	3	7	5	8.40	10.55	−17.03	undetermined
9	La Riera	RR1	Magdalenian	GI-1	NS	49	3	5	3	12.29	7.98	−18.29	undetermined
		RR4	Solutrean	LGM	NS	43	3	6	3	9.61	9.65	−17.43	undetermined
		RR9*	Solutrean	LGM	NS	45	3	3	3	15.11	6.08	−18.58	undetermined
		RR6	Solutrean	LGM	NS	41	3	3	3	13.56	5.54	−24.70	resident
11	Las Caldas	CL2	UM	GS-1	NS	41	3	5	6	7.47	9.14	−22.47	resident
		CL10	MM	GI-1	S	54	4	4	4	13.41	12.46	−16.87	undetermined
		CL21	Solutrean	LGM	S	36	4	3	3	11.92	7.46	−21.09	resident

the central portion of anadromous trout vertebra, and 11.0 ‰ ± 0.25 for river trout (Supplementary Fig. S3). As for $\delta^{13}C$, the difference in $\delta^{15}N$ values was significant only between the "anadromous trout adult stage" and resident trout group (Dunn test p-value = 0.0074).

3.6. Fork length, age and growth rate

FL was estimated for 219 brown trout (26 with and 192 without ecotype assignment, Supplementary Table S1) and ranged between 23.0 ± 3.4 cm and 60.7 ± 3.4 cm. Among the tested models for FL estimation, the bootstrap linear regression model was the best fitting for S and NS vertebrae, yielding R-squared values ranging between 0.83 (S vertebrae, M3) and 0.94 (NS vertebrae, M1, regression line shown in Fig. 8) and RSE between 3.4 and 5.6 cm. Previously published regression models resulted either less (r-squared between 0.64 and 0.89) or not at all (negative R-squared) suitable for our data. The different models tested and their estimated R-squared and residual standard error (RSE, i.e., the standard deviation of the residuals) are available in Supplementary Table S5.

Differences in FL across ecotypes were not significant (n = 26, Kruskal-Wallis test, p-values = 0.25, Spearman test [FL- $\delta^{13}C$], p-value = 0.16, Fig. 7b and Supplementary Fig. S4). Average FL in resident, undetermined and anadromous brown trout individuals were of 42.7 cm ± 4.81, 46.1 cm ± 4.47, and 47.9 cm ± 5.80, respectively. FL was significantly correlated with $\delta^{15}N$ (Spearman test, p-value = 0.0060, Supplementary Fig. S5).

The average FL during colder and warmer conditions (see Table 2) stood respectively at 42 ± 4 cm (n = 5) and 48 ± 3 cm (n = 1) in resident trout, 46 ± 4 cm (n = 9) and 47 ± 7 cm (n = 4) in "intermediate" samples, and 49 ± 7 cm (n = 9) and 45 ± 1 cm (n = 4) in anadromous samples. The effect of the climatic variable on FL could not be tested independently on each ecotype due to the low number of specimens within each. Overall, no significant effect of climate conditions on FL was detected when analysing the entire dataset (219 samples), which included individuals without ecotype classification. A subsampling approach was applied to account for the unbalanced distribution of data points by region and climatic conditions. For each 1000 iterations, 24 samples per region and condition combination were randomly selected, and the statistical analysis was repeated. The results showed no significant differences in FL by region or climatic conditions across these iterations.

Age was estimated for 211 samples. The average age ranged between 1 ± 0.6 to 7.5 ± 1.7 years (Fig. 9a and Supplementary Table S1). The MAE, calculated on the validation set, was globally 0.38 years, with an MAE of 0.52 and 0.15 years for the candid and expert readers, respectively (ages estimated by the two readers for the validation set are available in Supplementary Table S3). Inter-operator age variation yielded a CV of 12 % and 18 % for modern and archaeological samples, respectively.

Average GRs ranged between 6.00 and 30.5 cm/year. GR for resident, undetermined and anadromous samples were 11.6 ± 1.12 (n = 4), 15.6 ± 1.11 (n = 13) and 15.4 ± 2.11 (n = 14), respectively (Supplementary Fig. S4). The difference was not statistically significant. GR did not change significantly across space and time in the whole dataset.

Both FL and GR appeared significantly different in France during different periods. In France (Taillis des Coteaux, Troubat, and Duruthy), average FL was of 38.3 ± 5.1 (n = 25), 39.3 ± 6.6 (n = 27), 45.0 ± 8.2 (n = 6), 43.7 ± 11 (n = 9), and 44.1 ± 0 (n = 2), during pre-LGM, LGM, GI-1, GS-1 and interglacial Holocene period, respectively, and average GRs were of 13.1 ± 3.7 (n = 23), 10.8 ± 3.1 (n = 27), 13.9 ± 4.2 (n = 6), 16.9 ± 4.8 (n = 5), and 17.6 (n = 1). We observed a significant FL and GR increase after the LGM until the initial phases of the Holocene (Kruskal-Wallis p-value [FL] = 0.0090, Dunn test p-value [pre-LGM-post-LGM] = 0.0039, Dunn test p-value [LGM-post-LGM] = 0.032; Kruskal-Wallis p-value [GR] = 0.0046, Dunn test p-value [LGM-post-LGM] = 0.0030 Dunn test p-value [pre-LGM-LGM] = 0.042, Supplementary Fig. S6). In contrast, neither FL nor GR were significantly affected by climatic conditions (warm vs cold, as defined in Table 2) in either France or Spain.

4. Discussion

In the present study, we combined a range of biomolecular, chemical and biometric approaches to gather information on *S. trutta* life-history traits during the Pleistocene-Holocene transition. To our knowledge, this is the first time these methodologies are combined to address fish ecology during this period in Europe.

The results suggested a high diversity of *S. trutta* migratory strategies between 26 and 9 kyr B.P. Our $\delta^{13}C$ SIA values supported the hypothesis of a continuum of habitat use tactics, aligning with previous studies on contemporary Atlantic populations (Etheridge et al., 2008; Ruokonen et al., 2019). $\delta^{13}C$ values per each ecotype, including a range of "intermediate" values between resident and anadromous ecotypes (−18.6 ‰ to −16.5 ‰ in our sample and − 19.1 ‰ to −16.7 ‰ in Ruokonen et al., 2019), fell into the variability observed in modern populations. As expected, different ecotypes were featured with significantly different $\delta^{15}N$. No significant correlation between FL and GR was observed among fish with different ecotypes. However, in our dataset, fish of larger body size (FL > 50 cm) were non-resident. A positive significant correlation was found between FL and $\delta^{15}N$. All these results are consistent with data on modern facultative anadromous populations of brown trout in Northern Europe (e.g., Etheridge et al., 2008). Moreover, our data suggest a gradual FL and GR increase in France after the LGM until the beginning of the Holocene. On the other hand, FL and GR resulted unaffected by climatic conditions indicated in Table 2, in agreement with previous studies on early-middle Pleistocene brown trout samples (Blanco-Lapaz et al., 2021).

A crucial point of the study, that contrasts with previous studies of past brown trout ecology (Blanco-Lapaz et al., 2021; Kettle et al., 2011; Turrero et al., 2012) is the species authentication through ZooMS, allowing for an independent assessment of brown trout and Atlantic salmon ecology. ZooMS is able to deal with small-sized samples and has provided robust and reliable discrimination between these two species from the problematic *Salmo* genus once applied to minute fish vertebrae. To our knowledge, this is the first time that ZooMS has been used in Palaeolithic fish samples, offering a promising perspective for future studies. The ZooMS species discrimination on our samples showed that the size criterion is relevant to distinguishing *Salmo* species. Therefore, despite an only-partially-overlapping vertebral size ranges between *S. trutta* and *S. salar* (Fig. 5 and Supplementary Table S7), the size strategy could be applied when ZooMS analysis is unavailable. Nonetheless, it should be noted that the method presents some limitations. Large anadromous brown trout may be misidentified as Atlantic salmon, and conversely, it was not possible to distinguish pre-smolt Atlantic salmon from brown trout. Furthermore, in this study, only 27 vertebrae were identified as *S. salar* through ZooMS. Increasing the number of individuals would enhance the robustness of the method and help better assess its accuracy. A larger sample size would also permit to leverage NS and S vertebrae separately, refining the method, as vertebral size varies depending on the position along the rachis, as also observed in our dataset (Supplementary Table S7). Finally, beyond vertebral size, integrating information on the different size-at-age might further improve species discrimination, as previously suggested (e.g., Desse and Desse-Berset, 1992).

The range of carbon isotope values in archaeological collagen showed that Upper Palaeolithic *S. trutta* featured resident and anadromous populations. Our approach of combining a non-supervised and supervised ecotype classification method was all the more robust, as the archaeological collagen carbon isotope values fell within the same range of modern sample values (following tissue and Suess effect correction) and previous ichthyoarchaeological studies, as described below.

Using the unsupervised classification alone, 8 specimens (including

2 *S. salar*) were assigned as resident (range: −25.2 ‰ to −19.8 ‰), and 29, (including 9 *S. salar*), as anadromous (range: −18.6 ‰ to −12.3 ‰). While the resident signature was consistent with the $\delta^{13}C$ freshwater values reported in other ichthyoarchaeological studies (e.g., Guiry, 2019; Guiry et al., 2016a, 2016b), the marine signature was broader than expected. Although defying precise thresholds is difficult due to multiple confounding factors (Guiry, 2019), previous ichthyoarchaeological works observed $\delta^{13}C$ values $> \sim -16$ ‰ for marine environments (Guiry, 2019; Guiry et al., 2016a; Llorente-Rodríguez et al., 2022; Quinlan, 2023).

In contrast, the supervised model alone defined a freshwater range of −25.2 ‰ to −17.5 ‰, which did not align with previous studies. The integration of both methods produced the most reliable classification, yielding a range of −18.6 ‰ to −16.5 ‰ for the undetermined samples, with −16.3 ‰ representing the lowest marine value and − 19.9 ‰ the highest freshwater value.

Ecotype assignments based on carbon isotopes were further supported by significant differences in $\delta^{15}N$ values between ecotypes, mirroring patterns observed in modern populations (Etheridge et al., 2008). In our dataset, the fish with the highest FLs were anadromous, and overall, anadromous tended to exhibit greater FL than residents (Fig. 7b and Supplementary Fig. S4), albeit not statistically significant, possibly due to the small sample size ($n = 26$). Yet, the observed correlations between $\delta^{13}C$ and $\delta^{15}N$, and between $\delta^{15}N$ and FL, supported the tendency of undetermined and anadromous fish to display greater FLs.

Some intermediate values of $\delta^{13}C$ suggest that a substantial proportion of our ancient salmonids featured alternative migration patterns. Indeed, such values could be representative of either i) back-and-forth movements between coastal areas and the river, ii) a short (i.e., less than a year) lapse of coastal habitat occupation or iii) occupation of estuaries and/or low-salinity marine environments. Similar intermediate values -though in lower proportions- have been already documented on modern brown trout and have been interpreted as individuals with an intermediate life cycle, moving back and forth between marine/estuarine and riverine environments (Etheridge et al., 2008; Ruokonen et al., 2019). In our dataset, brown trout with "intermediate" $\delta^{13}C$ values and relatively low $\delta^{15}N$ values (e.g., RR1), could be interpreted as the result of late-migrations or intermittent periods of migration rather than brackish waters or "fully" anadromous individuals, living under low-salinity conditions at sea, as one would expect higher values of $\delta^{15}N$ for either brackish waters or "fully" anadromous individuals of that age and FL (Table 3 and Supplementary Fig. S5). Other samples, such as MR1, have $\delta^{15}N$, FL, and age values consistent with these two interpretations (i.e., late/intermittent migrants or ecotone denizens), together with the third hypothesis of being fully anadromous fish living in low-salinity conditions -if dated from the post-LGM period, like CL10 (Table 3). Carbon isotope collagen values rely on collagen turnover, which, to the best of our knowledge, has not been fully documented in fish (Ankjærø et al., 2012; Guiry and Hunt, 2020; Matsubayashi et al., 2017). Therefore, it is likely that movements within periods below a year, which have been reported in the literature for salmonids (Orell et al., 2018), might not translate into full marine signatures. Such behaviour has been well documented in the northernmost distribution of brown trout (Northern Scandinavia), where anadromous brown trout is found to spend an extended period (almost 2 years) in freshwater before and after spawning, even though the feeding status during this period is still debated (Lähteenmäki et al., 2025). A wide range of intermediate carbon isotopes collagen values might also reflect differences in the duration of the juvenile stage in freshwater prior to migration into seawater, as seen in some modern contexts (Ferguson et al., 2019). Seaward migration appeared to be a size-dependent trait (Ferguson et al., 2019), meaning that the growth rate determines the time required to reach a particular size threshold. The age at migration has been found to depend on latitude and river size (e.g., Økland et al., 1993). In Norway, brown trout from southern rivers (latitude 60°/61° N) spend 2–3 years in freshwater whereas this stage rises to 3–6 years in northern rivers (latitude c. 67°N; Økland et al., 1993). The wide range of age estimations in our intermediate and anadromous fish might thus be evidence of varying lengths of the juvenile stage in freshwater before migration (Fig. 7c).

In migratory fish, the collagen deposited during the freshwater stages differs isotopically from that deposited in seawater (Doucett et al., 1999a, 1999b; McCarthy and Waldron, 2000) and this signal can be differentially measured by analysing separately different portions of the vertebra (e.g., Matsubayashi et al., 2017, 2019) Despite our limited sample, our data on vertebrae from contemporary sea trout confirmed that collagen turnover was sufficiently slow to preserve isotopic signatures from different life stages. In our archaeological specimens, alas, separating the juvenile stage from the sea occupation phase was impossible due to the scant collagen yield. While the lifelong collagen was analysed in bulk, discrimination of freshwater and marine water occupancy was obtained in line with modern values. The mixture between signatures of different life stages, however, must be considered when interpreting fish intermediate carbon isotope signatures, which likely reflect migratory individuals that spent a variable number of years in freshwater before migrating to the sea -thus blurring the overall carbon signal. On the other hand, fish growth during the marine phase is usually higher than in the freshwater phase and this is reflected in the calcified structures (e.g., Baglinière et al., 2020).

Another factor to consider when interpreting SIA $\delta^{13}C$ values for inferring migratory life history is the mixing of freshwater and seawater (e.g., brackish water; Fry, 2002; Strøm et al., 2021). Indeed, the assignment of the resident ecotype to two *S. salar* individuals during the post-LGM stage (Fig. 6b) could be attributed to the occupation of a marine habitat under the influence of large freshwater influxes. Substantial freshwater influx into the marine environment due to ice melting between 18 and 11 kyr B.P., has been well-documented in palaeoclimatological studies and resulted in lower salinity levels (minimal salinity at −16 kyr B.P.), at least on a local scale (Ménot et al., 2006). Alternative hypotheses of salmon freshwater residency appear less likely; in modern contexts, river resident salmon exhibit much smaller sizes (Birt et al., 1991; Hutchings et al., 2019) than the two freshwater-assigned individuals of our study (85 ± 4 cm and 69 ± 4 cm, see Supplementary Table S1). Lake-migratory Atlantic salmon can reach higher body lengths but, to our knowledge, no big lakes have been documented for the hydrologic basins of these two *S. salar* individuals (Lea and Nalon river for Santa Catalina and Las Caldas respectively, see Supplementary File A). At the same time, we cannot rule out a different freshwater system during the Late Palaeolithic, especially after the LGM when the glaciers discharge might have formed bigger aquatic basins. A scenario where river residency allowed Atlantic salmon to reach FL > 50 cm seems less likely considering the available data on modern river-resident Atlantic salmon but cannot be excluded. Overall, the hypothesis of Atlantic salmon migrating towards low-salinity areas appears the most plausible, as such environments have been documented during deglaciation and might have been highly productive due to glacial discharge (Hopwood et al., 2020; Meire et al., 2017). For instance, some authors consider the Channel an extended glacial river during this period (e.g., Kettle et al., 2011; Ménot et al., 2006). Therefore, *S. trutta* ecotype assignment during the ice-melting period could reflect biases towards freshwater occupancy and/or intermediate life histories. However, it is important to notice that the model presented here for ecotype assignment was calibrated on brown trout samples, which have different ecology compared to Atlantic salmon. This may have biased out interpretation of *S. salar* samples.

Such facts notwithstanding, the resident ecotype found during the LGM, provided strong evidence of the presence of this ecotype together with other migratory ecotypes during the transition from the LGM towards milder conditions. Considering all elements, the "intermediate" fish best fit a migratory life cycle -either estuarine or marine, with the latter being more strongly substantiated by the possible scenarios outlined here. However, the presence of freshwater individuals falling

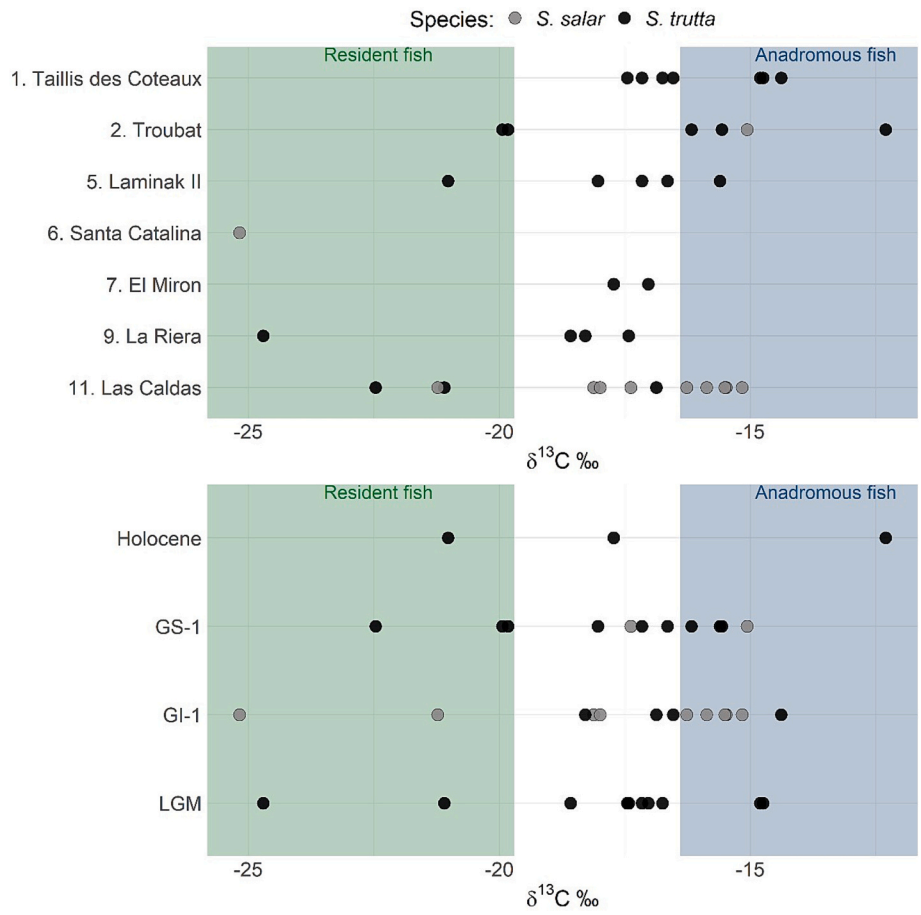

Fig. 6. Carbon isotope values distribution for *S. trutta* and *S. salar* per site (upper panel) and period (lower panel). Periods are assigned according to Table 2. GS and GI stand for Greenland stadial and interstadial and represent colder and warmer phases of the North Atlantic region, respectively. (For interpretation of the references to colour in this figure legend, the reader is referred to the web version of this article.)

outside the expected freshwater range cannot be excluded, as supported by the literature (e.g., Guiry et al., 2020). Indeed, many factors influence $\delta^{13}C$ and despite trying to create a classification model that helps to clarify the framework, this might come at the cost of over-simplification.

The main limitation of both models lies in their attempt to represent a system that is intrinsically difficult to model. Interpreting carbon and nitrogen isotope signatures ideally requires local and period-specific baseline values, which are unavailable for archaeological samples. Hence, a trade-off was necessary. One approach was using multiple contemporaneous specimens and grouping them based on isotopic similarity, as implemented in our clustering analysis. Alternatively, modern datasets can provide freshwater and marine reference ranges based on known ecotypes. In this second case, the reference ranges are necessarily broader due to geographical variability, and may not accurately reflect past environmental conditions. The clustering method does not account for local conditions as, owing to the limited number of specimens, could not be applied separately for each site or basin, potentially leading to misclassification. The generalised model, on the other hand, may leave samples unassigned when their values fall in overlapping ranges between freshwater and marine signatures. This ambiguity can arise from intermediate life-history traits, or alternatively, from a shift in the local isotopic baseline, pushing both reference signatures towards the extremes. In conclusion, despite its limitations, the combined approach represented for this study the best trade-off for interpreting $\delta^{13}C$ values. Nonetheless, final ecotype assignments should always be supported by additional life-history traits such as FL, age, growth rate, and $\delta^{15}N$.

The difference of ~5 ‰ between the two peaks in the anadromous $\delta^{15}N$ distribution was higher than the typical difference between two trophic levels (Alexandre, 2020; Drucker et al., 2018), suggesting either a high degree of intraspecific trophic diversity in the marine environment or else an occupation of two different habitats at sea with very contrasted trophic food webs. As the specimens from these two groups came from different sites (i.e., 1 individual from Laminak II [$\delta^{15}N$ = 13.9 ‰], 3 from Troubat [average $\delta^{15}N$ = 14 ‰ ± 1.82] and 3 from Taillis des Coteaux [average $\delta^{15}N$ = 9.16 ‰ ± 0.044]), the latter hypothesis seems more probable. Published data evidenced significant $\delta^{15}N$ variation associated with marine locations (e.g., inshore, offshore) and latitude (Chouvelon et al., 2015; Hansen et al., 2012). In addition, our modern reference datasets, including published and newly generated data in our study, revealed differences of 3–5 ‰ across different locations in Europe. As already claimed in previous studies (Guiry, 2019; Katzenberg, 1989), these considerations underline that caution is needed when interpreting $\delta^{15}N$ values as direct indicators of trophic behaviour without the appropriate context (e.g., $\delta^{15}N$ values of primary producers through amino acids, etc.). For anadromous brown trout, conditions in the marine domain would have been rather variable through time during the period under consideration. The presence of two resident-assigned *S. salar* in two Spanish sites in simultaneous periods (Las Caldas and Santa Catalina) in post-LGM periods could evidence temporally and spatially restricted large freshwater discharges into the coastal areas.

Regarding fish length and age estimations, a novelty of our models and protocols is that they were calibrated on a large number of samples (n ~ 50) exclusively composed of brown trout modern reference samples. In addition, to the best of our knowledge, this is the first study

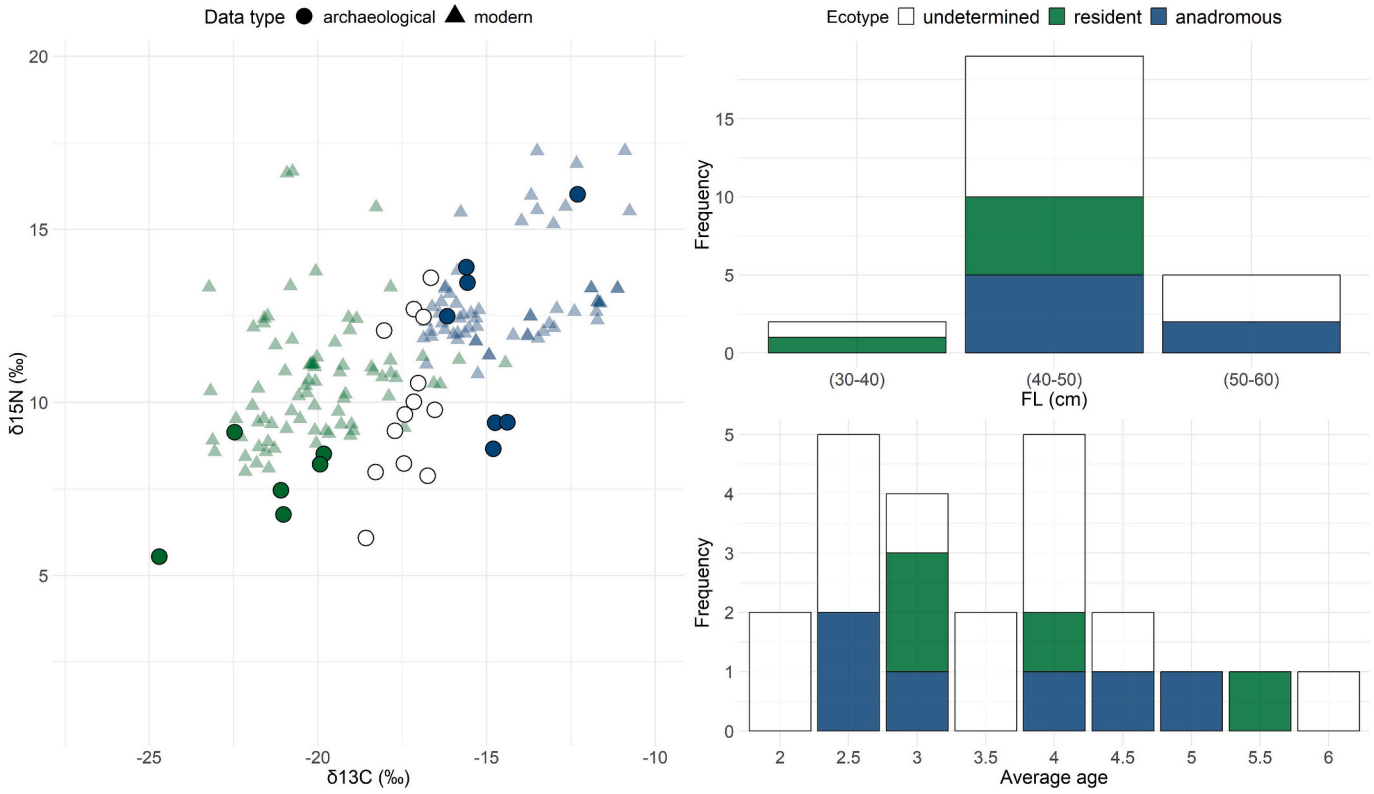

Fig. 7. Ecotype, fork length and age of 26 Upper Palaeolithic brown trout. *S. trutta* ecotype assignment and relative stable isotope analysis (SIA) values (dots in the left panel), fork length (FL) range (upper right panel) and age range (lower right panel) of archaeological brown trout ($n = 26$). Triangles (left panel) represent carbon and nitrogen SIA values of themodern reference dataset ($n = 114$) used for ecotype classification through the supervised model and the ensemble of the modern samples ($N = 15$) generated in this study (also represented in Supplementary Fig. S3). (For interpretation of the references to colour in this figure legend, the reader is referred to the web version of this article.)

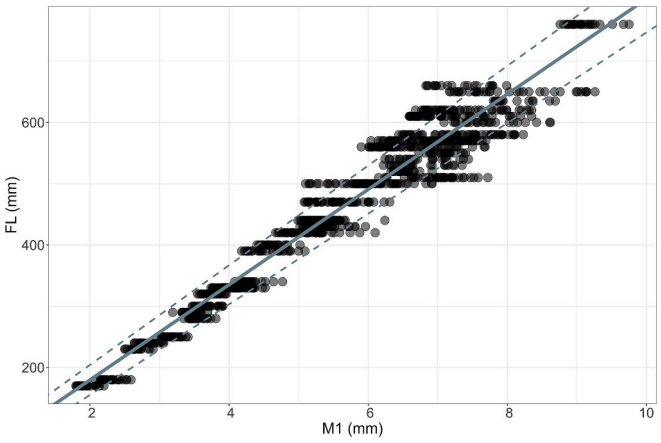

Fig. 8. Allometric regression models (FL ~ M1, non-spinous [NS] vertebrae type). The plot shows the bootstrap (1000 replicates) linear regression model for M1 and vertebra type NS (R-squared = 0.94 and RSE = 3.4 cm). The x-axis represents the vertebrae dimension M1 of the 49 modern brown trout used to generate the model, while the y-axis represents FL per each individual. Each individual has > 20 vertebrae of NS type. The line represents the average regression lines obtained through bootstrap. The dashed lines represent the confidence interval of 95 % for the parameters (intercept and slope) of the regression line. (For interpretation of the references to colour in this figure legend, the reader is referred to the web version of this article.)

where the variability within a group of vertebrae of the same type (e.g., NS and S) is accounted for (see Supplementary Table S5 for more details on the sampling and approach used to generate the regression models).

This may explain why the published regression models for body length estimation in *S. trutta* tested on our modern brown trout dataset were less accurate than ours (Supplementary Table S5).

The accuracy and precision of our models were higher for M1 and M2 than for M3, which might be explained in part by the fact that, in brown trout, vertebral number is variable and vertebral thickness (M3) depends on the number of vertebrae.

Our method for annuli interpretation is based on the study of modern brown trout vertebrae and scales. The involvement of both an expert and a candid reader enabled us to assess the protocol's viability. Despite the MAE of the candid reader being low (0.52 years), it is advisable that the analysis is carried out by a reader with experience in sclerochronology as the distance from the real age decreases drastically (MAE = 0.15).

In contrast with some previous studies (Blanco-Lapaz and Vergès, 2016; Desse and Desse-Berset, 1992; Turrero et al., 2012), in ours, readers could not interpret the vertebral edge and core for the season of capture and migratory status in archaeological samples, despite this was possible for modern samples. Further studies might throw light on this issue.

FL, age and growth rates of our archaeological specimens fell within the range of modern brown trout populations in Europe (e.g., Nevoux et al., 2019, Fig. 9b; Ruokonen et al., 2019). Despite the low number of specimens with an inferred ecotype, the FL range of Palaeolithic brown trout (41–56 cm, 38–54 cm and 36–48 cm for anadromous, intermediate and resident ecotypes respectively, Table 3) fall within the range of modern northern European equivalents (37–78 cm, 26–59 cm and 27–73 cm for anadromous, intermediate and resident brown trout, in Ruokonen et al., 2019). However, the absence of brown trout on the margins of this range (< 23 cm and > 61 cm) might be due to different reasons. Small fish species have been deemed unidentified to avoid misidentification of juveniles of Atlantic salmon (section 2.3). On the

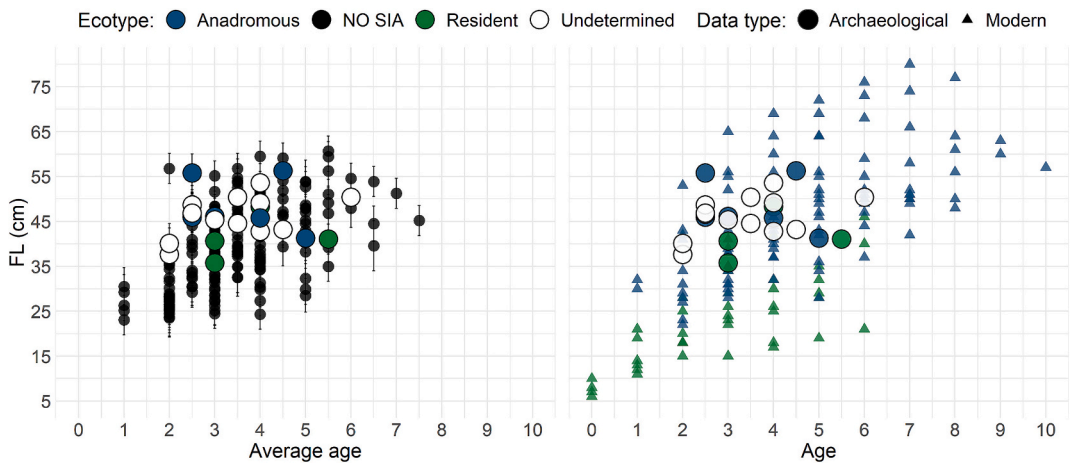

Fig. 9. FL and age distribution of 219 Upper Palaeolithic brown trout and contemporary brown trout. The left panel displays the FL distribution (with relative error) and average age distribution of 219 brown trout archaeological samples, including those without ecotype assignment (black). The right panel shows FL and age distribution of contemporary resident (green) and anadromous (blue) brown trout previously published (Nevoux et al., 2019) together with the 23 (6 anadromous, in blue, 4 resident, in green, and 13 intermediate, in white) archaeological brown trout for which ecotype, FL and age was estimated in this study (Table 3). (For interpretation of the references to colour in this figure legend, the reader is referred to the web version of this article.)

other hand, big brown trout might have been less common in the past, although one tends to think that the opposite would hold as high fishing pressure is known to reduce the maximum body lengths of fish in general (e.g., Limburg et al., 2008). In addition, exceptionally large vertebrae of brown trout might have been assigned to Atlantic salmon, as species identification in the case of non-ZooMS-analysed specimens was based on vertebral dimensions of samples identified through ZooMS. The analysis of further vertebrae of salmonids through ZooMS should help refine our model.

The statistical analyses concerning FL and climatic conditions (warm vs cold, as defined in Table 2) confirmed the results from previous studies reporting that the temperature shifts during the Pleistocene did not determine variation in brown trout body lengths (Blanco-Lapaz et al., 2021). However, other factors (such as population density, predators, sample accumulator factors, etc) might skew this result.

During the deglaciation, greater FLs and GRs in brown trout populations from the French region possibly reflect higher contrast between the LGM and post-LGM conditions in France than in the Iberian Peninsula.

In our study, anadromous brown trout were predominantly found in the Northern margin of the Iberian glacial refugia (northern to the Pyrenees, i.e., Taillis Des Coteaux and Troubat), as originally hypothesised by Roselló Izquierdo (1989) and later by Leal García (2014). This is significant, as the propensity to migrate of anadromous trout enables dispersion and might have driven the (re-)colonisation of post-LGM environments. The presence of anadromous fish, together with improved growth conditions favouring larger sizes, provided conditions for the expansion of trout ranges towards northern Europe during post-glacial times (Cortés-Guzmán et al., 2024; Ferguson, 2006; Jarry et al., 2018). The hypothesis that post-LGM colonisers derived mostly from the northern margins of the glacial refugium could be tested through genetic analysis.

The present study provides insights into fishing activities during the Pleistocene-Holocene transition. Although no analysis of butchery marks was undertaken, a human or mixed accumulation has been hypothesised for most of the archaeological sites (Guillaud, 2014; Marín-Arroyo et al., 2023; Roselló-Izquierdo and Morales-Muñiz, 2014). By contrast, non-human predators might be central in fishbone accumulation in Aitzbitarte III and Laminak II (Roselló and Brinkhuizen, 1994; Roselló Izquierdo and Morales Muñiz, 2011a; Rosello-Izquierdo and Morales Muniz, 2016). Still, the role played by non-human fish accumulators in northern Iberian archaeological sites has not been pursued systematically through taphonomic analyses, with some exceptions (Morales Muniz, 1984; Roselló and Brinkhuizen, 1994; Roselló Izquierdo and Morales Muñiz, 2011b; Roselló-Izquierdo and Morales-Muñiz, 2014, 2017). The presence of anadromous fish on inland sites, in turn, suggests that these were likely targeted by nomadic humans acquainted with the seasonal migrations of the animals. This particularly stands for those archaeological sites further inland (e.g., Taillis Des Coteaux and Troubat, see Fig. 1), which interestingly are the ones with the higher proportion of anadromous brown trout. If present-day trends constitute valid analogues for interpretation, then one may assume that anadromous migrations coincided with the colder months of the year (Elliott, 1994). This would turn salmonids into a crucial fall-back resource when alternative foodstuffs were scarce, and more so if their meat could be processed for delayed consumption. Year-round availability of resident freshwater fish, in turn, would make these reliable targets and a dietary supplement when anadromous fish were absent or scarce. Our study reveals that this dual reliance on both anadromous and resident fish hints at a strategic resource utilisation approach to optimising fish availability throughout the year.

Even though sampling of the archaeological collection was stratified to include different vertebral sizes, biases due to the way archaeological excavations have been carried out (e.g., Zohar and Belmaker, 2005) and a size selection due to the accumulator are intrinsic to the sample. Moreover, part of the present study relied on collagen extracted from fish vertebrae. The selection criterion based on vertebrae weight (Fig. 3) restricted the incorporation of the smallest fish, potentially introducing additional size-related biases into the dataset. Although 57 % of the samples collected were above the weight threshold of 35 mg (Supplementary Table S1) that we considered reasonable for such old samples, only ~10 % yielded collagen that meet the quality criteria required for ZooMS and SIA. Indeed, low success rates have been observed in similar archaeological fish studies (e.g., Robson et al., 2016). The small and porous nature of *Salmo* spp. vertebrae, as well as the mineral and collagen structure of fish bones in general, may significantly influence collagen preservation (Szpak, 2011). In particular, the high % of lipid content of fish might have compromised the collagen quality of some of the archaeological samples with high C:N ratio and low $\delta^{13}C$ values (Guiry, Szpak, et al., 2016, see Supplementary Fig. S1). Samples used in the present study were far older than those of equivalent studies in fish, and this might seriously compromise collagen preservation.

Another issue with the present work concerns the limited number of samples with reliable SIA restricting the power of the statistical analyses.

This limitation is more relevant when one considers the multiple factors to test for (e.g., climatic events, archaeological contexts, cultural periods, etc.). Our samples cover a long temporal window, during which multiple climatic events took place, and derive from a good number of archaeological sites. Whereas this aspect represented an interesting novelty of our study and was originally planned, it also posed challenges in terms of interpretation due to the restricted number of specimens with meaningful SIA results. Grouping climatic events into broad categories (i.e., cold vs warm; Table 2) and archaeological sites in terms of macro-regions (France vs Spain), helped us interpret the results but risks over-simplifying matters.

One final possible bias to consider is using modern data as a reference to study archaeological samples. Despite this being a suitable strategy for both FL estimation and ecotype identification (coupled with the interpretation based only on the archaeological values in the latter case), also been used in previous studies (e.g., Andrews et al., 2022; E. Guiry et al., 2020; Turrero et al., 2012), we cannot assume that the food webs and environmental conditions remained stable over time and overlook the bias possibly introduced. To minimise this issue, we diversified as much as possible the datasets, including fish from different aquatic basins and with different ecotypes, sizes, ages, and sexes for dataset S3 and fish from different latitudes and climatic conditions for the dataset used to generate the supervised model for ecotype identification.

5. Conclusion

The present study provides insights into brown trout phenotypic variation during the Pleistocene-Holocene transition, a critical period for life's evolutionary history. Our findings underscore the adaptative response of brown trout to environmental changes, thanks to its high phenotypic diversity, in terms of life-history strategies, diet, and size at maturity, which we found held on throughout the period under consideration.

Supplementary data to this article can be found online at https://doi.org/10.1016/j.palaeo.2025.113073.

CRediT authorship contribution statement

Ambra D'Aurelio: Writing – review & editing, Writing – original draft, Software, Resources, Project administration, Methodology, Investigation, Funding acquisition, Formal analysis, Data curation, Conceptualization. **Lucía Agudo Pérez:** Writing – review & editing, Writing – original draft, Methodology, Investigation, Formal analysis. **Lawrence G. Straus:** Writing – review & editing, Writing – original draft, Resources. **Manuel R. González Morales:** Visualization, Validation, Resources. **Arturo Morales-Muñiz:** Writing – review & editing, Resources. **Jerome Primault:** Writing – original draft, Visualization, Validation, Resources. **Jean-Marc Roussel:** Writing – review & editing, Resources. **Laurence Tissot:** Writing – review & editing, Validation. **Stephane Glise:** Validation, Resources, Methodology. **Frederic Lange:** Validation, Methodology, Formal analysis. **Camille Riquier:** Visualization, Software, Methodology, Formal analysis. **Michel Barbaza:** Writing – original draft, Visualization, Resources. **Eduardo Berganza:** Writing – original draft, Visualization. **José Luis Arribas:** Writing – original draft, Visualization. **Pablo Arias:** Writing – original draft, Visualization. **Aurélien Simonet:** Writing – original draft, Visualization. **Ana B. Marín-Arroyo:** Writing – review & editing, Visualization, Validation, Supervision, Resources, Methodology, Conceptualization. **Joelle Chat:** Writing – review & editing, Visualization, Validation, Supervision, Resources, Project administration, Methodology, Investigation, Funding acquisition, Data curation, Conceptualization. **Françoise Daverat:** Writing – review & editing, Writing – original draft, Visualization, Validation, Supervision, Software, Resources, Project administration, Methodology, Investigation, Funding acquisition, Conceptualization.

Declaration of competing interest

The authors declare that they have no known competing financial interests or personal relationships that could have appeared to influence the work reported in this paper.

Acknowledgements

We thank Jean-Christophe Aymes, Emmanuel Huchet and Jean-Marc Teulé for their technical support. We are grateful to Philippe Béarez for insightful discussions and training in salmonid osteology and allometry. We appreciate the valuable suggestions on ZooMS interpretation provided by Liz Quinlan and Leire Torres-Iglesias. The collection of specimens for the osteotheque was made possible thanks to Aurélie Flesselle and Quentin Josset; Yoann Guilloux, Nicolas Jeannot, and Fabien Quendo; Jean-Claude Etchegoyen; Pedro Leunda; and the French National Federation of Fishing (Fédération Nationale de Pêche), who provided the contemporary samples of brown trout and Atlantic salmon. We thank them all. We are grateful for the constructive comments and edits from E. Guiry and the three anonymous reviewers. The authors would also like to thank SILVATECH (SILVATECH, 2018) 10.15454/1.5572400113627854E12 from UMR 1434 SILVA, 1136 IAM, 1138 BEF and 4370 EA LERMAB from the research center INRAE Grand-Est Nancy for it contribution to isotopic analysis, elementary analysis and methodological development. SILVATECH facility is supported by the French National Research Agency through the Laboratory of Excellence ARBRE (ANR-11-LABX-0002-01). For the scales and vertebrae (image and reading), we benefited from the assistance of the technical platform of the IE ECP (ECP, 2018).

This research has received funding from the European Union's Horizon 2020 research and innovation programme under the Marie Skłodowska-Curie grant agreement N° 945416, as well as from the *Communauté d'Agglomération Pau Béarn Pyrénées* and the EDF (*Électricité de France*), contract N° 5925205104, and the European Research Council under the European Union's Horizon 2020 Research and Innovation Programme grant agreement N° 818299 (SUBSILIENCE project; https://www.subsilience.eu).

Data availability

The data presented in this work are available in Supplementary Material. In addition, the datasets of modern skeletons used as a reference for allometric and sclerochronological analyses are publicly accessible at: https://entrepot.recherche.data.gouv.fr/dataset.xhtml?persistentId=doi:10.57745/EC2IGO&version=1.0

References

Acolas, M.L., Labonne, J., Baglinière, J.L., Roussel, J.M., 2012. The role of body size versus growth on the decision to migrate: a case study with Salmo trutta. Naturwissenschaften 99 (1), 11–21. https://doi.org/10.1007/s00114-011-0861-5.

Adán, G.E., Álvarez-Lao, D., Turrero, P., Arbizu, M., García-Vázquez, E., 2009. Fish as diet resource in North Spain during the Upper Paleolithic. J. Archaeol. Sci. 36 (3), 895–899. https://doi.org/10.1016/j.jas.2008.11.017.

Alexandre, P., 2020. Isotopes and the Natural Environment. Springer International Publishing. https://doi.org/10.1007/978-3-030-33652-3.

Allentoft, M.E., Collins, M., Harker, D., Haile, J., Oskam, C.L., Hale, M.L., Campos, P.F., Samaniego, J.A., Gilbert, M.T.P., Willerslev, E., Zhang, G., Scofield, R.P., Holdaway, R.N., Bunce, M., 2012. The half-life of DNA in bone: measuring decay kinetics in 158 dated fossils. Proc. R. Soc. B Biol. Sci. 279 (1748), 4724–4733. https://doi.org/10.1098/rspb.2012.1745.

Álvarez-Fernández, E., 2011. Humans and marine resource interaction reappraised: Archaeofauna remains during the late Pleistocene and Holocene in Cantabrian Spain. J. Anthropol. Archaeol. 30 (3), 327–343. https://doi.org/10.1016/j.jaa.2011.05.005.

Ambrose, S.H., 1990. Preparation and characterization of bone and tooth collagen for isotopic analysis. J. Archaeol. Sci. 17 (4), 431–451. https://doi.org/10.1016/0305-4403(90)90007-R.

Andrews, A.J., Mylona, D., Rivera-Charún, L., Winter, R., Onar, V., Siddiq, A.B., Tinti, F., Morales-Muniz, A., 2022. Length estimation of Atlantic bluefin tuna (Thunnus

thynnus) using vertebrae. Int. J. Osteoarchaeol. 32 (3), 645–653. https://doi.org/10.1002/oa.3092.
Ankjærø, T., Christensen, J., Grønkjær, P., 2012. Tissue-specific turnover rates and trophic enrichment of stable N and C isotopes in juvenile Atlantic cod Gadus morhua fed three different diets. Mar. Ecol. Prog. Ser. 461, 197–209. https://doi.org/10.3354/meps09871.
Baglinière, J.L., Hamelet, V., Guéraud, F., Aymes, J.C., Goulon, C., Richard, A., Josset, Q., Marchand, F., 2020. Guide to the Interpretation of the Scales and the Estimation of the Age of Brown Trout (*Salmo trutta*) from the French Populations. Guides and. Ed.
Birt, T.P., Green, J.M., Davidson, W.S., 1991. Mitochondrial DNA variation reveals genetically distinct sympatric populations of anadromous and nonanadromous Atlantic Salmon, Salmo salar. Can. J. Fish. Aquat. Sci. 48 (4), 577–582. https://doi.org/10.1139/f91-073.
Blanco-Lapaz, À., Vergès, J.M., 2016. Fish remains from the Neolithic site of El Mirador cave (Atapuerca, Spain): seasonality and resource management. Comptes Rendus Palevol 15 (6), 745–751. https://doi.org/10.1016/j.crpv.2015.09.007.
Blanco-Lapaz, A., Martínez-Monzón, A., Blain, H.-A., Cuenca-Bescós, G., 2021. Early-Middle Pleistocene freshwater ecosystems in the Sierra de Atapuerca (northern Iberia) based on the Gran Dolina fish record. Palaeogeogr. Palaeoclimatol. Palaeoecol. 574, 110444. https://doi.org/10.1016/j.palaeo.2021.110444.
Buckley, M., Collins, M.J., 2011. Collagen survival and its use for species identification in Holocene-lower Pleistocene bone fragments from British archaeological and paleontological sites. Antiqua 1 (1), Article 1. https://doi.org/10.4081/antiqua.2011.e1.
Buckley, M., Collins, M., Thomas-Oates, J., Wilson, J.C., 2009. Species identification by analysis of bone collagen using matrix-assisted laser desorption/ionisation time-of-flight mass spectrometry. Rapid Commun. Mass Spectrom. 23 (23), 3843–3854. https://doi.org/10.1002/rcm.4316.
Buckley, M., Harvey, V.L., Petiffer, D., Russ, H., Wouters, W., Van Neer, W., 2022. Medieval fish remains on the Newport ship identified by ZooMS collagen peptide mass fingerprinting. Archaeol. Anthropol. Sci. 14 (3), 41. https://doi.org/10.1007/s12520-021-01478-y.
Casteel, R.W., 1976. Fish remains in archaeology and paleo-environmental studies. Academic Press. https://cir.nii.ac.jp/crid/1130000794661667328.
Cersoy, S., Zazzo, A., Lebon, M., Rofes, J., Zirah, S., 2017. Collagen Extraction and Stable Isotope Analysis of Small Vertebrate Bones: A Comparative Approach. Radiocarbon 59 (3), 679–694. https://doi.org/10.1017/RDC.2016.82.
Charles, K., Roussel, J.-M., Cunjak, R.A., 2004. Estimating the contribution of sympatric anadromous and freshwater resident brown trout to juvenile production. Mar. Freshw. Res. 55 (2), 185. https://doi.org/10.1071/MF03173.
Chouvelon, T., Schaal, G., Grall, J., Pernet, F., Perdriau, M., A-Pernet, E.J., Le Bris, H., 2015. Isotope and fatty acid trends along continental shelf depth gradients: Inshore *versus* offshore hydrological influences on benthic trophic functioning. Prog. Oceanogr. 138, 158–175. https://doi.org/10.1016/j.pocean.2015.07.013.
Clark, P.U., Dyke, A.S., Shakun, J.D., Carlson, A.E., Clark, J., Wohlarth, B., Mitrovica, J. X., Hostetler, S.W., McCabe, A.M., 2009. The Last Glacial Maximum. Science 710–714.
Consuegra, S., García De Leániz, C., Serdio, A., González Morales, M., Straus, L.G., Knox, D., Verspoor, E., 2002. Mitochondrial DNA variation in Pleistocene and modern Atlantic salmon from the Iberian glacial refugium. Mol. Ecol. 11 (10), 2037–2048. https://doi.org/10.1046/j.1365-294X.2002.01592.x.
Cortés-Guzmán, D., Sinclair, J., Hof, C., Kalusche, J.B., Haase, P., 2024. Dispersal, glacial refugia and temperature shape biogeographical patterns in European freshwater biodiversity. Glob. Ecol. Biogeogr. 33 (9), e13886. https://doi.org/10.1111/geb.13886.
Cortey, M., Vera, M., Pla, C., García-Marín, J.-L., 2009. Northern and Southern expansions of Atlantic brown trout (Salmo trutta) populations during the Pleistocene: phylogeography of Atlantic brown trout. Biol. J. Linn. Soc. 97 (4), 904–917. https://doi.org/10.1111/j.1095-8312.2009.01220.x.
Dawson, T.P., Jackson, S.T., House, J.I., Prentice, I.C., Mace, G.M., 2011. Beyond predictions: biodiversity conservation in a changing climate. Science 332 (6025), 53–58. https://doi.org/10.1126/science.1200303.
DeNiro, M.J., 1985. Postmortem preservation and alteration of in vivo bone collagen isotope ratios in relation to palaeodietary reconstruction. Nature 317 (6040). https://doi.org/10.1038/317806a0. Article 6040.
Desse, J., Desse-Berset, N., 1992. Age et saison de mort des poissons: Applications à l'archéologie. Squelettochronologie (Poissons) 341–353.
Doucett, R.R., Hooper, W., Power, G., 1999a. Identification of anadromous and nonanadromous adult brook trout and their progeny in the Tabusintac River, New Brunswick, by means of multiple-stable-isotope analysis. Trans. Am. Fish. Soc. 128 (2), 278–288. https://doi.org/10.1577/1548-8659(1999)128<0278:IOAANA>2.0.CO;2.
Doucett, R.R., Power, M., Power, G., Caron, F., Reist, J.D., 1999b. Evidence for anadromy in a southern relict population of Arctic charr from North America. J. Fish Biol. 55 (1), 84–93. https://doi.org/10.1111/j.1095-8649.1999.tb00658.x.
Drucker, D.G., Valentin, F., Thevenet, C., Mordant, D., Cottiaux, R., Delsate, D., Van Neer, W., 2018. Aquatic resources in human diet in the Late Mesolithic in Northern France and Luxembourg: insights from carbon, nitrogen and sulphur isotope ratios. Archaeol. Anthropol. Sci. 10 (2), 351–368. https://doi.org/10.1007/s12520-016-0356-6.
ECP, INRAE, 2018. Ecology and Fish Population Biology Facility. https://doi.org/10.15454/1.5572402068944548E12.
Elliott, J.A., 1994. Quantitative Ecology and the Brown Trout. Oxford University Press. https://academic.oup.com/book/53245.
Etheridge, E.C., Harrod, C., Bean, C., Adams, C.E., 2008. Continuous variation in the pattern of marine v. Freshwater foraging in brown trout Salmo trutta L. from Loch Lomond, Scotland. J. Fish Biol. 73 (1), 44–53. https://doi.org/10.1111/j.1095-8649.2008.01905.x.
Feltham, M.J., Marquiss, M., 1989. The use of first vertebrae in separating, and estimating the size of, trout (Salmo trutta) and salmon (Salmo salar) in bone remains. J. Zool. 219 (1), 113–122. https://doi.org/10.1111/j.1469-7998.1989.tb02570.x.
Ferguson, A., 2006. Genetics of sea trout, with particular reference to Britain and Ireland. In: Sea Trout: Biology, Conservation and Management, 1st ed. John Wiley & Sons, Ltd., pp. 157–182. https://doi.org/10.1002/9780470996027
Ferguson, A., Reed, T.E., Cross, T.F., McGinnity, P., Prodöhl, P.A., 2019. Anadromy, potamodromy and residency in brown trout *Salmo trutta*: the role of genes and the environment. J. Fish Biol. 95 (3), 692–718. https://doi.org/10.1111/jfb.14005.
Fordham, D.A., Jackson, S.T., Brown, S.C., Huntley, B., Brook, B.W., Dahl-Jensen, D., Gilbert, M.T.P., Otto-Bliesner, B.L., Svensson, A., Theodoridis, S., Wilmshurst, J.M., Buettel, J.C., Canteri, E., McDowell, M., Orlando, L., Pilowsky, J.A., Rahbek, C., Nogues-Bravo, D., 2020. Using paleo-archives to safeguard biodiversity under climate change. Science 369 (6507), eabc5654. https://doi.org/10.1126/science.abc5654.
Fry, B., 2002. Conservative mixing of stable isotopes across estuarine salinity gradients: a conceptual framework for monitoring watershed influences on downstream fisheries production. Estuaries 25 (2), 264–271. https://doi.org/10.1007/BF02691313.
Fry, B., Sherr, E.B., 1984. Δ13C measurements as indicators of carbon flow in marine and freshwater ecosystems. Contributions in Marine Science 27, 13–47.
Fuller, B.T., Van Neer, W., Linseele, V., De Cupere, B., Chahoud, J., Richards, M.P., 2020. Fish δ13C and δ15N results from two Bronze/Iron Age sites (Tell Tweini & Sidon) along the Levantine coast. J. Archaeol. Sci. Rep. 29, 102066. https://doi.org/10.1016/j.jasrep.2019.102066.
Gibb, S., Strimmer, K., 2012. MALDIquant: a versatile R package for the analysis of mass spectrometry data. Bioinformatics 28 (17), 2270–2271. https://doi.org/10.1093/bioinformatics/bts447.
Goodwin, J.C.A., Andrew King, R., Iwan Jones, J., Ibbotson, A., Stevens, J.R., 2016. A small number of anadromous females drive reproduction in a brown trout (Salmo trutta) population in an English chalk stream. Freshw. Biol. 61 (7), 1075–1089. https://doi.org/10.1111/fwb.12768.
Gregory, S.D., Armstrong, J.D., Britton, J.R., 2018. Is bigger really better? Towards improved models for testing how Atlantic salmon *Salmo salar* smolt size affects marine survival. J. Fish Biol. 92 (3), 579–592. https://doi.org/10.1111/jfb.13550.
Gruber, N., Keeling, C.D., Bacastow, R.B., Guenther, P.R., Lueker, T.J., Wahlen, M., Meijer, H.A.J., Mook, W.G., Stocker, T.F., 1999. Spatiotemporal patterns of carbon-13 in the global surface oceans and the oceanic suess effect. Glob. Biogeochem. Cycles 13 (2), 307–335. https://doi.org/10.1029/1999GB900019.
Guillaud, E., 2014. Études archéo-ichtyofaunique des sites magdaléniens du Taillis des Coteaux et de La Piscine (Vallée de la Gartempe, Vienne): Taphonomie, biodiversité et techniques de pêche [These de doctorat, Paris, Muséum national d'histoire naturelle]. https://theses.fr/2014MNHN0021.
Guillaud, E., Cornette, R., Béarez, P., 2016. Is vertebral form a valid species-specific indicator for salmonids? The discrimination rate of trout and Atlantic salmon from archaeological to modern times. J. Archaeol. Sci. 65, 84–92. https://doi.org/10.1016/j.jas.2015.11.010.
Guiry, E.J., 2019. Complexities of stable carbon and nitrogen isotope biogeochemistry in ancient freshwater ecosystems: implications for the study of past subsistence and environmental change. Front. Ecol. Evol. 7. https://doi.org/10.3389/fevo.2019.00313.
Guiry, E.J., Hunt, B.P.V., 2020. Integrating fish scale and bone isotopic compositions for 'deep time' retrospective studies. Mar. Environ. Res. 160, 104982. https://doi.org/10.1016/j.marenvres.2020.104982.
Guiry, E.J., Robson, H.K., 2024. Deep antiquity of seagrasses supporting European eel fisheries in the western Baltic. Proc. R. Soc. B Biol. Sci. 291 (2027), 20240674. https://doi.org/10.1098/rspb.2024.0674.
Guiry, E.J., Szpak, P., 2020. Quality control for modern bone collagen stable carbon and nitrogen isotope measurements. Methods Ecol. Evol. 11 (9), 1049–1060. https://doi.org/10.1111/2041-210X.13433.
Guiry, E.J., Szpak, P., 2021. Improved quality control criteria for stable carbon and nitrogen isotope measurements of ancient bone collagen. J. Archaeol. Sci. 132, 105416. https://doi.org/10.1016/j.jas.2021.105416.
Guiry, E.J., Needs-Howarth, S., Friedland, K.D., Hawkins, A.L., Szpak, P., Macdonald, R., Courtemanche, M., Holm, E., Richards, M.P., 2016a. Lake Ontario salmon (Salmo salar) were not migratory: a long-standing historical debate solved through stable isotope analysis. Sci. Rep. 6 (1). https://doi.org/10.1038/srep36249. Article 1.
Guiry, E.J., Szpak, P., Richards, M.P., 2016b. Effects of lipid extraction and ultrafiltration on stable carbon and nitrogen isotopic compositions of fish bone collagen. Rapid Commun. Mass Spectrom. 30 (13), 1591–1600.
Guiry, E.J., Royle, T.C.A., Matson, R.G., Ward, H., Weir, T., Waber, N., Brown, T.J., Hunt, B.P.V., Price, M.H.H., Finney, B.P., Kaeriyama, M., Qin, Y., Yang, D.Y., Szpak, P., 2020. Differentiating salmonid migratory ecotypes through stable isotope analysis of collagen: archaeological and ecological applications. PLoS One 15 (4), e0232180. https://doi.org/10.1371/journal.pone.0232180.
Halffman, C.M., Potter, B.A., McKinney, H.J., Finney, B.P., Rodrigues, A.T., Yang, D.Y., Kemp, B.M., 2015. Early human use of anadromous salmon in North America at 11,500 y ago. Proc. Natl. Acad. Sci. 112 (40), 12344–12348. https://doi.org/10.1073/pnas.1509747112.
Hansen, J., Hedeholm, R., Sünksen, K., Christensen, J., Grønkjær, P., 2012. Spatial variability of carbon (δ^{13} C) and nitrogen (δ^{15N}) stable isotope ratios in an Arctic

marine food web. Mar. Ecol. Prog. Ser. 467, 47–59. https://doi.org/10.3354/meps09945.
Harvey, V.L., Daugnora, L., Buckley, M., 2018. Species identification of ancient Lithuanian fish remains using collagen fingerprinting. J. Archaeol. Sci. 98, 102–111. https://doi.org/10.1016/j.jas.2018.07.006.
Hayden, B., Chisholm, B., Schwarcz, H.P., 1987. Fishing and foraging. Marine resources in the Upper Paleolithic of France. In: Soffer, O. (Ed.), The Pleistocene Old World. Springer US, pp. 279–291. https://doi.org/10.1007/978-1-4613-1817-0_18.
Hewitt, G., 2000. The genetic legacy of the Quaternary ice ages. Nature 405 (6789), 907–913. https://doi.org/10.1038/35016000.
Hodson, T.O., 2022. Root-mean-square error (RMSE) or mean absolute error (MAE): when to use them or not. Geosci. Model Dev. 15 (14), 5481–5487. https://doi.org/10.5194/gmd-15-5481-2022.
Holmes, K.M., Robson Brown, K.A., Oates, W.P., Collins, M.J., 2005. Assessing the distribution of African Palaeolithic sites: a predictive model of collagen degradation. J. Archaeol. Sci. 32 (2), 157–166. https://doi.org/10.1016/j.jas.2004.06.002.
Hopwood, M.J., Carroll, D., Dunse, T., Hodson, A., Holding, J.M., Iriarte, J.L., Ribeiro, S., Achterberg, E.P., Cantoni, C., Carlson, D.F., Chierici, M., Clarke, J.S., Cozzi, S., Fransson, A., Juul-Pedersen, T., Winding, M.H.S., Meire, L., 2020. Review article: How does glacier discharge affect marine biogeochemistry and primary production in the Arctic? The Cryosphere 14 (4), 1347–1383. https://doi.org/10.5194/tc-14-1347-2020.
Hutchings, J.A., Ardren, W.R., Barlaup, B.T., Bergman, E., Clarke, K.D., Greenberg, L.A., Lake, C., Piironen, J., Sirois, P., Sundt-Hansen, L.E., Fraser, D.J., 2019. Life-history variability and conservation status of landlocked Atlantic salmon: An overview, p. 76.
Jarry, M., Beall, E., Davaine, P., Guéraud, F., Gaudin, P., Aymes, J.-C., Labonne, J., Vignon, M., 2018. Sea trout (Salmo trutta) growth patterns during early steps of invasion in the Kerguelen Islands. Polar Biol. 41 (5), 925–934. https://doi.org/10.1007/s00300-018-2253-1.
Jones, J.R., Marín-Arroyo, A.B., Straus, L.G., Richards, M.P., 2020. Adaptability, resilience and environmental buffering in European Refugia during the Late Pleistocene: insights from La Riera Cave (Asturias, Cantabria, Spain). Sci. Rep. 10 (1), 1217. https://doi.org/10.1038/s41598-020-57715-2.
Jones, J.R., Marín-Arroyo, A.B., Corchón Rodríguez, M.S., Richards, M.P., 2021. After the Last Glacial Maximum in the refugium of northern Iberia: environmental shifts, demographic pressure and changing economic strategies at Las Caldas Cave (Asturias, Spain). Quat. Sci. Rev. 262, 106931. https://doi.org/10.1016/j.quascirev.2021.106931.
Jonsson, N., Jonsson, B., 2007. Sea growth, smolt age and age at sexual maturation in Atlantic salmon. J. Fish Biol. 71 (1), 245–252. https://doi.org/10.1111/j.1095-8649.2007.01488.x.
Jonsson, B., L'Abée-Lund, J.H., 1993. Latitudinal clines in life-history variables of anadromous brown trout in Europe. J. Fish Biol. 43 (sA), 1–16. https://doi.org/10.1111/j.1095-8649.1993.tb01175.x.
Kahn, G.R., Pearson, E.D., Dick, J.E., 2004. Comparison of standard length, fork length, and total length for measuring west coast marine fishes. Mar. Fish. Rev. 66 (1), 31.
Katzenberg, M.A., 1989. Stable isotope analysis of archaeological faunal remains from Southern Ontario. J. Archaeol. Sci. 16 (3), 319–329. https://doi.org/10.1016/0305-4403(89)90008-3.
Kettle, A.J., Morales-Muñiz, A., Roselló-Izquierdo, E., Heinrich, D., Vøllestad, L.A., 2011. Refugia of marine fish in the Northeast Atlantic during the last glacial maximum: concordant assessment from archaeozoology and palaeotemperature reconstructions. Clim. Past 7 (1), 181–201. https://doi.org/10.5194/cp-7-181-2011.
Korzow Richter, K., Wilson, J., Jones, A.K.G., Buckley, M., van Doorn, N., Collins, M.J., 2011. Fish 'n chips: ZooMS peptide mass fingerprinting in a 96 well plate format to identify fish bone fragments. J. Archaeol. Sci. 38 (7), 1502–1510. https://doi.org/10.1016/j.jas.2011.02.014.
Korzow Richter, K., McGrath, K., Masson-MacLean, E., Hickinbotham, S., Tedder, A., Britton, K., Bottomley, Z., Dobney, K., Hulme-Beaman, A., Zona, M., Fischer, R., Collins, M.J., Speller, C.F., 2020. What's the catch? Archaeological application of rapid collagen-based species identification for Pacific Salmon. J. Archaeol. Sci. 116, 105116. https://doi.org/10.1016/j.jas.2020.105116.
Lähteenmäki, L., Huusko, R., Hellström, G., Snickars, M., Romakkaniemi, A., 2025. Two-year spawning migration as a life-history strategy of sea trout (L.) in large, high-latitude river systems. Ecol. Freshw. Fish 34 (2), e70002. https://doi.org/10.1111/eff.70002.
Lambeck, K., Rouby, H., Purcell, A., Sun, Y., Sambridge, M., 2014. Sea level and global ice volumes from the Last Glacial Maximum to the Holocene. Proc. Natl. Acad. Sci 111 (43), 15296–15303. https://doi.org/10.1073/pnas.1411762111.
Le Gall, O., 1984. L'ichtyofaune d'eau douce dans les sites préhistoriques: Ostéologie-paléoécologie-paléoethnologie. FeniXX.
Leal García, M.S., 2014. Variabilidad genética y filogeografía de la trucha común 'Salmo trutta' en el sur de la Península Ibérica [Http://purl.org/dc/dcmitype/Text, Universidad Complutense de Madrid]. In: Variabilidad genética y filogeografía de la trucha común 'Salmo trutta' en el sur de la Península Ibérica. https://produccioncientifica.ucm.es/documentos/5d1df61729995204f7661058?lang=fr.
LeRoy Poff, N., Day, J.W., Brinson, M.M., 2002. Aquatic Ecosystems & Global Climate Change – Potential Impacts on Inland Freshwater and Coastal Wetland Ecosystems in the United States, 44. Pew Center on Global Climate Change, pp. 1–36.
Letcher, B.H., Gries, G., 2003. Effects of life history variation on size and growth in stream-dwelling Atlantic salmon. J. Fish Biol. 62 (1), 97–114. https://doi.org/10.1046/j.1095-8649.2003.00009.x.
Limburg, K.E., Walther, Y., Hong, B., Olson, C., Storå, J., 2008. Prehistoric versus modern Baltic Sea cod fisheries: selectivity across the millennia. Proc. R. Soc. B Biol. Sci. 275 (1652), 2659–2665. https://doi.org/10.1098/rspb.2008.0711.
Llorente-Rodríguez, L., Craig, O.E., Colonese, A.C., von Tersch, M., Roselló-Izquierdo, E., Gómez, González, de Agüero, E., Fernández-Rodríguez, C., Quirós-Castillo, J.A., López-Arias, B., Marlasca-Martín, R., Nottingham, J., Morales Muñiz, A., 2022. Elucidating historical fisheries' networks in the Iberian Peninsula using stable isotopes. Fish Fish. 23 (4), 862–873. https://doi.org/10.1111/faf.12655.
Longin, R., 1971. New method of collagen extraction for radiocarbon dating. Nature 230 (5291), 241–242. https://doi.org/10.1038/230241a0.
Magri, D., Vendramin, G.G., Comps, B., Dupanloup, I., Geburek, T., Gömöry, D., Latałowa, M., Litt, T., Paule, L., Roure, J.M., Tantau, I., Van Der Knaap, W.O., Petit, R.J., De Beaulieu, J.-L., 2006. A new scenario for the Quaternary history of European beech populations: palaeobotanical evidence and genetic consequences. New Phytol. 171 (1), 199–221. https://doi.org/10.1111/j.1469-8137.2006.01740.x.
Marín-Arroyo, A.B., Geiling, J.M., Jones, E.L., Carvalho, M., Gonzalez Morales, M.R., Straus, L.G., 2023. Seasonality of human occupations in El Mirón Cave: Late Upper Paleolithic Hunter-Gatherer settlement-subsistence systems in Cantabrian Spain. J. Paleolithic Archaeol. 6 (1), 7. https://doi.org/10.1007/s41982-022-00134-8.
Matsubayashi, J., Saitoh, Y., Osada, Y., Uehara, Y., Habu, J., Sasaki, T., Tayasu, I., 2017. Incremental analysis of vertebral centra can reconstruct the stable isotope chronology of teleost fishes. Methods Ecol. Evol. 8 (12), 1755–1763. https://doi.org/10.1111/2041-210X.12834.
Matsubayashi, J., Umezawa, Y., Matsuyama, M., Kawabe, R., Mei, W., Wan, X., Shimomae, A., Tayasu, I., 2019. Using segmental isotope analysis of teleost fish vertebrae to estimate trophic discrimination factors of bone collagen. Limnol. Oceanogr. Methods 17 (2), 87–96. https://doi.org/10.1002/lom3.10298.
McCarthy, I.D., Waldron, S., 2000. Identifying migratory Salmo trutta using carbon and nitrogen stable isotope ratios. Rapid Commun. Mass Spectrom. 14 (15), 1325–1331. https://doi.org/10.1002/1097-0231(20000815)14:15<1325::AID-RCM980>3.0.CO;2-A.
Meire, L., Mortensen, J., Meire, P., Juul-Pedersen, T., Sejr, M.K., Rysgaard, S., Nygaard, R., Huybrechts, P., Meysman, F.J.R., 2017. Marine-terminating glaciers sustain high productivity in Greenland fjords. Glob. Change Biol. 23 (12), 5344–5357. https://doi.org/10.1111/gcb.13801.
Meiri, M., Lister, A.M., Higham, T.F.G., Stewart, J.R., Straus, L.G., Obermaier, H., González Morales, M.R., Marín-Arroyo, A.B., Barnes, I., 2013. Late-glacial recolonization and phylogeography of European red deer (ervus elaphus L.). Mol. Ecol. 22 (18), 4711–4722. https://doi.org/10.1111/mec.12420.
Ménot, G., Bard, E., Rostek, F., Weijers, J.W.H., Hopmans, E.C., Schouten, S., Damsté, J. S.S., 2006. Early reactivation of European Rivers during the last deglaciation. Science 313 (5793), 1623–1625. https://doi.org/10.1126/science.1130511.
Miller, J.D., Robert, N.L., 1972. Guide to the Coastal Marine Fishes of California.
Mion, L., André, T., Mailloux, A., Sternberg, M., Morales Muniz, A., Rosello-Izquierdo, E., Llorente Rodríguez, L., Herrscher, E., 2022. Contribution to Mediterranean medieval dietary studies: stable carbon and nitrogen isotope data of marine and catadromous fish from Provence (9th–14th CE). Data Brief 41, 108016. https://doi.org/10.1016/j.dib.2022.108016.
Miszaniec, J.I., 2021. Assessing past ecological tolerance of Pacific salmon (Oncorhynchus spp.) and saffron cod (Eleginus gracilis) in Northwest Alaska using vertebra width and length reconstructions | Archaeological and Anthropological Sciences. Archaeol. Anthropol. Sci. 13 (6), 1–24.
Morales, A., 1984. A study of the representativity and taxonomy of the fish faunas from two Mousterian sites on northern Spain with special reference to the trout, pp. 41–59.
Morales Muniz, A., 1984. Primer informe sobre la ictiofauna magdaleniense de la Cueva de Tito Bustillo (provincia de Asturias). Primer Informe Sobre La Ictiofauna Magdaleniense de La Cueva de Tito Bustillo (Provincia de Asturias) 38 (113), 903–930.
Morales Muñiz, A., Roselló-Izquierdo, E., 2016. Fishing in Mediterranean prehistory: An archaeo-ichthyological overview. In: The Inland Seas: Towards an Ecohistory of the Mediterranean and the Black Sea, vol. 35. Franz Steiner Verlag. https://doi.org/10.25162/9783515114431.
Morales Muniz, A., Rosenlund, K., 1979. Fish Bone Measurements. An Attempt to Standardize the Measuring of Fish Bones from Archaeological Sites. Stennstrupia, Copenhague.
Morales Muñiz, A., Frontini, R., Fernández-Jalvo, Y., Roselló-Izquierdo, E., Pesquero-Fernández, M.D., Hernández, A.B., García, L.A., 2021. Evaluation of size-related salmonid fish vertebrae deformation due to compression: an experimental approach. Archaeol. Anthropol. Sci. 13 (12), 215.
Morales-Muñiz, A., Roselló-Izquierdo, E., 2008. 20,000 years of fishing in the Strait: Archaeological fish and shellfish assemblages from southern Iberia. In: Human Impacts on Ancient Marine Environments. University of California Press, pp. 243–278. https://cir.nii.ac.jp/crid/1370565169357833360.
Morales-Muñiz, A., Llorente-Rodríguez, L., Rosello-Izquierdo, E., 2021. Fish bone studies in Iberia: An overview of 40 years of research from the LAZ-UAM (Madrid). In: Themes in Old World Archaeozoology: From the Mediterranean to the Atlantic. Oxbow Books, pp. 173–188. https://doi.org/10.2307/j.ctv13pk8dp.6.
Nevoux, M., Finstad, B., Davidsen, J.G., Finlay, R., Josset, Q., Poole, R., Höjesjö, J., Aarestrup, K., Persson, L., Tolvanen, O., Jonsson, B., 2019. Environmental influences on life history strategies in partially anadromous brown trout (Salmo trutta, Salmonidae). Fish Fish. 20 (6), 1051–1082. https://doi.org/10.1111/faf.12396.
Økland, F., Jonsson, B., Jensen, A.J., Hansen, L.P., 1993. Is there a threshold size regulating seaward migration of brown trout and Atlantic salmon? J. Fish Biol. 42 (4), 541–550. https://doi.org/10.1111/j.1095-8649.1993.tb00358.x.
Opel, T., Bertran, P., Grosse, G., Jones, M., Luetscher, M., Schirrmeister, L., Stadelmaier, K., Veremeeva, A., 2024. Ancient permafrost and past permafrost in the Northern Hemisphere. In: Elias, S.A. (Ed.), *Encyclopedia of Quaternary Science*, 3rd Edition. Elsevier. https://doi.org/10.1016/B978-0-323-99931-1.00258-0.

Orell, P., Erkinaro, J., Kiljunen, M., Torniainen, J., Sutela, T., Jaukkuri, M., Mäki-Petäys, A., 2018. Short sea migration and precocious maturation in reared Atlantic salmon post-smolts in the northern Baltic Sea. ICES J. Mar. Sci. 75 (3), 1063–1070. https://doi.org/10.1093/icesjms/fsx213.

Owens, N.J.P., 1985. Variations in the natural abundance of 15N in estuarine suspended particulate matter: A specific indicator of biological processing. Estuarine. Coastal and Shelf Science 20 (4), 505–510. https://doi.org/10.1016/0272-7714(85)90092-7.

Post, D.M., Layman, C.A., Arrington, D.A., Takimoto, G., Quattrochi, J., Montaña, C.G., 2007. Getting to the fat of the matter: Models, methods and assumptions for dealing with lipids in stable isotope analyses. Oecologia 152 (1), 179–189. https://doi.org/10.1007/s00442-006-0630-x.

Prenda, J., Arenas, M.P., Freitas, D., Santos-Reis, M., Collares-Pereira, M.J., 2002. Estimation of prey fish size consumed by piscivores. Limnetica 21 (1–2), 15–24.

Quay, P., Sonnerup, R., Stutsman, J., Maurer, J., Körtzinger, A., Padin, X.A., Robinson, C., 2007. Anthropogenic CO2 accumulation rates in the North Atlantic Ocean from changes in the 13C/12C of dissolved inorganic carbon. Glob. Biogeochem. Cycles 21 (1). https://doi.org/10.1029/2006GB002761.

Quinlan, L.M., 2023. Medieval Ichthyoarchaeology and Historical Ecology of Salmo sp. Fishes Across the North Sea Basin [Phd, University of York]. https://etheses.whiterose.ac.uk/35247/.

R Core Team, 2023. R: A language and environment for statistical computing (Version 4.2.3) [Computer software]. Foundation for Statistical Computing. https://www.r-project.org.

Rasmussen, S.O., Bigler, M., Blockley, S.P., Blunier, T., Buchardt, S.L., Clausen, H.B., Cvijanovic, I., Dahl-Jensen, D., Johnsen, S.J., Fischer, H., Gkinis, V., Guillevic, M., Hoek, W.Z., Lowe, J.J., Pedro, J.B., Popp, T., Seierstad, I.K., Steffensen, J.P., Svensson, A.M., Winstrup, M., 2014. A stratigraphic framework for abrupt climatic changes during the Last Glacial period based on three synchronized Greenland ice-core records: refining and extending the INTIMATE event stratigraphy. Quat. Sci. Rev. 106, 14–28. https://doi.org/10.1016/j.quascirev.2014.09.007.

Robson, H.K., Andersen, S.H., Clarke, L., Craig, O.E., Gron, K.J., Jones, A.K.G., Karsten, P., Milner, N., Price, T.D., Ritchie, K., Zabilska-Kunek, M., Heron, C., 2016. Carbon and nitrogen stable isotope values in freshwater, brackish and marine fish bone collagen from Mesolithic and Neolithic sites in central and northern Europe. Environ. Archaeol. https://doi.org/10.1179/1749631415Y.0000000014.

Roselló, E., Brinkhuizen, D., 1994. Laminak II / Spain: alternative taxonomies as approaches to the interpretation of a fish fauna. Offa 51, 401–409.

Roselló Izquierdo, E., 1989. Arqueoictiofaunas ibéricas aproximación metodológica y bio-cultural. Http://purl.org/dc/dcmitype/Text. Universidad Autónoma de Madrid. https://dialnet.unirioja.es/servlet/tesis?codigo=37278.

Roselló Izquierdo, E., Morales Muñiz, A., 2011a. Estudio de los peces del yacimiento de Aitzbitarte III (zona de entrada). Ocupaciones humanas en Aitzbitarte III (País Vasco) 33.600-18.400 BP: Zona de entrada a la cueva, 2011, ISBN 978-84-457-3216-8, págs. 507-516, 507–516. https://dialnet.unirioja.es/servlet/articulo?codigo=8246950.

Roselló Izquierdo, E., Morales Muñiz, A., 2011b. Evidencias de pesca en las ocupaciones de Santimamiñe. Kobie. Bizkaiko Arkeologi Indusketak = Excavaciones Arqueológicas en Bizkaia 1, 239–246.

Rosello-Izquierdo, E., Morales Muniz, A., 2016. Los peces Gravetienses de la zona interior de la Cueva de Aitzbitarte III. In: Ocupaciones Humanas en Aitzbitarte III.

Roselló-Izquierdo, E., Morales-Muñiz, A., 2014. Las ictiofaunas de Santa Catalina (Lequeitio, Vizcaya): Un registro singular para la prehistoria cantábrica. Kobie Serie Bizkaiko Arkeologi Indusketak, Excavaciones Arqueologicas en *Bizkaia*(4), 161–262.

Roselló-Izquierdo, E., Morales-Muñiz, A., 2017. Los peces de la cueva de Praileaitz I (Deba, Gipuzkoa). Munibe Monogr. 1, 327–331. https://doi.org/10.21630/mmaas.2017.1.11.

Roselló-Izquierdo, E., Berganza-Gochi, E., Nores-Quesada, C., Morales-Muñiz, A., 2016. Santa Catalina (Lequeitio, Basque Country): an ecological and cultural insight into the nature of prehistoric fishing in Cantabrian Spain. J. Archaeol. Sci. Rep. 6, 645–653. https://doi.org/10.1016/j.jasrep.2015.06.002.

Ruokonen, T.J., Kiljunen, M., Erkinaro, J., Orell, P., Sivonen, O., Vestola, E., Jones, R.I., 2019. Migration strategies of brown trout (Salmo trutta) in a subarctic river system as revealed by stable isotope analysis. Ecol. Freshw. Fish 28 (1), 53–61. https://doi.org/10.1111/eff.12426.

Saloniemi, I., Jokikokko, E., Kallio-Nyberg, I., Jutila, E., Pasanen, P., 2004. Survival of reared and wild Atlantic salmon smolts: size matters more in bad years. ICES J. Mar. Sci. 61 (5), 782–787. https://doi.org/10.1016/j.icesjms.2004.03.032.

SILVATECH, INRAE, 2018. Structural and functional analysis of tree and wood Facility. https://doi.org/10.15454/1.5572400113627854E12.

Stadelmaier, K.H., Ludwig, P., Bertran, P., Antoine, P., Shi, X., Lohmann, G., Pinto, J.G., 2021. A new perspective on permafrost boundaries in France during the Last Glacial Maximum. Climate of the Past 17 (6), 2559–2576. https://doi.org/10.5194/cp-17-2559-2021.

Strohalm, M., 2023. MMass: A Free Mass Spectrometry Tool (Version 5.5.0) [Computer software]. MMass Development Team. http://www.mmass.org.

Strøm, J.F., Jensen, J.L.A., Nikolopoulos, A., Nordli, E., Bjørn, P.A., Bøhn, T., 2021. Sea trout Salmo trutta in the subarctic: Home-bound but large variation in migratory behaviour between and within populations. J. Fish Biol. 99 (4), 1280–1291. https://doi.org/10.1111/jfb.14832.

Szpak, P., 2011. Fish bone chemistry and ultrastructure: Implications for taphonomy and stable isotope analysis. J. Archaeol. Sci. 38 (12), 3358–3372. https://doi.org/10.1016/j.jas.2011.07.022.

Thieren, E., Wouters, W., Van Neer, W., Ervynck, A., 2012. Body length estimation of the European eel Anguilla anguilla on the basis of isolated skeletal elements. Cybium 551–562.

Turrero, P., Horreo, J.L., Garcia-Vazquez, E., 2012. Same old Salmo? Changes in life history and demographic trends of North Iberian salmonids since the Upper Palaeolithic as revealed by archaeological remains and beast analyses. Mol. Ecol. 21 (10), 2318–2329. https://doi.org/10.1111/j.1365-294X.2012.05508.x.

Turrero, P., García-Vázquez, E., de Leaniz, C.G., 2014. Shrinking fish: Comparisons of prehistoric and contemporary salmonids indicate decreasing size at age across millennia. R. Soc. Open Sci. 1 (2), 140026. https://doi.org/10.1098/rsos.140026.

van Doorn, N.L., Hollund, H., Collins, M.J., 2011. A novel and non-destructive approach for ZooMS analysis: ammonium bicarbonate buffer extraction. Archaeol. Anthropol. Sci. 3 (3), 281–289. https://doi.org/10.1007/s12520-011-0067-y.

Van Neer, W., Löugas, L., Rijnsdorp, A.D., 1999. Reconstructing age distribution, season of capture and growth rate of fish from archaeological sites based on otoliths and vertebrae. Int. J. Osteoarchaeol. 9 (2), 116–130. https://doi.org/10.1002/(SICI)1099-1212(199903/04)9:2<116::AID-OA465>3.0.CO;2-H.

Verburg, P., 2007. The need to correct for the Suess effect in the application of δ13C in sediment of autotrophic Lake Tanganyika, as a productivity proxy in the Anthropocene. J. Paleolimnol. 37 (4), 591–602. https://doi.org/10.1007/s10933-006-9056-z.

Vitale, F., Worsøe Clausen, L., Ní Chonchúir, G., 2019. Handbook of fish age estimation protocols and validation methods [Report]. ICES Cooperative Research Reports (CRR). https://doi.org/10.17895/ices.pub.5221.

Watt, J., Pierce, G.J., Boyle, P.R., 1997. Guide to the identification of North Sea fish using Premaxillae and Vertebrae [Report]. ICES Cooperative Research Reports (CRR). https://doi.org/10.17895/ices.pub.4627.

Welker, F., Soressi, M., Rendu, W., Hublin, J.-J., Collins, M., 2015. Using ZooMS to identify fragmentary bone from the Late Middle/arly Upper Palaeolithic sequence of Les Cottés, France. J. Archaeol. Sci. 54, 279–286. https://doi.org/10.1016/j.jas.2014.12.010.

Zohar, I., Belmaker, M., 2005. Size does matter: Methodological comments on sieve size and species richness in fishbone assemblages. J. Archaeol. Sci. 32 (4), 635–641. https://doi.org/10.1016/S0305-4403(03)00037-2.

Update

Palaeogeography, Palaeoclimatology, Palaeoecology
Volume 675, Issue , 1 October 2025, Page

DOI: https://doi.org/10.1016/j.palaeo.2025.113113

Palaeogeography, Palaeoclimatology, Palaeoecology 675 (2025) 113113

Contents lists available at ScienceDirect

Palaeogeography, Palaeoclimatology, Palaeoecology

journal homepage: www.elsevier.com/locate/palaeo

Corrigendum to "Phenotypic diversity of brown trout (*Salmo trutta* L.) during the late Upper Pleistocene and Early Holocene in the glacial refugium of Iberia" [Palaeogeography, Palaeoclimatology, Palaeoecology (2025) 113073]

Ambra D'Aurelio [a,*], Lucía Agudo Pérez [b], Lawrence G. Straus [b,c], Manuel R. González Morales [d], Arturo Morales-Muñiz [e], Jerome Primault [f], Jean-Marc Roussel [g], Laurence Tissot [h], Stephane Glise [a], Frederic Lange [a], Camille Riquier [a], Michel Barbaza [i], Eduardo Berganza [j], José Luis Arribas [k], Pablo Arias [d], Aurélien Simonet [l], Ana B. Marín-Arroyo [b], Joelle Chat [a], Françoise Daverat [a]

[a] *Université de Pau et des Pays de l'Adour, INRAE, UMR ECOBIOP, Saint-Pée-sur-Nivelle, France*
[b] *Grupo I+D+I EvoAdapta, Dpto. de Ciencias Históricas, Universidad de Cantabria, Santander, Spain*
[c] *Department of Anthropology, MSC01 1040, University of New Mexico, Albuquerque, NM 87131-0001, USA*
[d] *Instituto Internacional de Investigaciones Prehistóricas de Cantabria, Universidad de Cantabria, Gobierno de Cantabria, Santander, Spain*
[e] *Laboratorio de Arqueozoología (LAZ-UAM)-Universidad Autónoma de Madrid, Darwin, 2, Madrid, Spain*
[f] *DRAC/SRA, Nouvelle-Aquitaine, Ministry of Culture and Communications, Poitiers, France*
[g] *DECOD (Ecosystem Dynamics and Sustainability), Institut Agro, INRAE, IFREMER, Rennes, France*
[h] *EDF R&D, LNHE (Laboratoire National d'Hydraulique et Environnement), 6 Quai Watier, Chatou 78401, France*
[i] *TRACES UMR 5608, CNRS, UT2J Université de Toulouse Jean-Jaures, France*
[j] *Sociedad de Ciencias Aranzadi, Donostia/San Sebastián, Spain*
[k] *AOZTA, Bilbao, Spain*
[l] *Service de la conservation des musées & du patrimoine, Direction de la culture et du patrimoine, Mont-de-Marsan, France*

In this article the following paragraph was omitted from the Acknowledgements section, "Many thanks to Cesar Garcia de Castro and Antonia Pedregal Montes at the Museo Arqueológico de Asturias; Iñaki García Camino and Joseba Rios Garaizar at the Arkeologia Museoa Bilbao; Sonia San Jose at Centro de Colecciones Patrimoniales de Bienes Muebles de Gipuzkoa (Gordailua); Roberto Ontañon and Adriana Chauvin at the Museo de Arqueología y Prehistoria de Cantabria (MUPAC); to Delphine Haro-Gabay at the Musée d'Histoire et d'Archéologie de l'Abbaye d'Arthous du département des Landes and to Cristina San Juan-Foucher at the Service Régional de l'Archéologie DRAC d'Occitanie for facilitating access to their collections. We are particularly grateful for the welcome received at these museums and their help during the sampling and permission processes." The original article has been corrected.

The authors would like to apologise for any inconvenience caused.

DOI of original article: https://doi.org/10.1016/j.palaeo.2025.113073.
* Corresponding author at: INRAE UMR 1224 ECOBIOP, 64310, Saint Pée sur Nivelle, France.
E-mail address: ambra.d-aurelio@inrae.fr (A. D'Aurelio).

https://doi.org/10.1016/j.palaeo.2025.113113

Available online 8 July 2025